Biogeosciences, 19, 1–27, 2022
https://doi.org/10.5194/bg-19-1-2022

Biogeosciences Open Access EGU

An analysis of the variability in $\delta^{13}C$ in macroalgae from the Gulf of California: indicative of carbon concentration mechanisms and isotope discrimination during carbon assimilation

Roberto Velázquez-Ochoa[1], María Julia Ochoa-Izaguirre[2], and Martín Federico Soto-Jiménez[3]

[1]Posgrado en Ciencias del Mar y Limnología, Unidad Académica Mazatlán, Universidad Nacional Autónoma de México, Mazatlán, Sinaloa 82040, México
[2]Facultad de Ciencias del Mar, Universidad Autónoma de Sinaloa, Paseo Claussen s/n, Mazatlán, Sinaloa 82000, México
[3]Instituto de Ciencias del Mar y Limnología, Unidad Académica Mazatlán, Universidad Nacional Autónoma de México (UAM-ICMyL-UNAM), Mazatlán, Sinaloa 82040, México

Correspondence: Martín Federico Soto-Jiménez (martin@ola.icmyl.unam.mx)

Received: 24 February 2021 – Discussion started: 9 March 2021
Revised: 25 October 2021 – Accepted: 9 November 2021 – Published: 3 January 2022

Abstract. The isotopic composition of carbon in macroalgae ($\delta^{13}C$) is highly variable, and its prediction is complex concerning terrestrial plants. The determinants of $\delta^{13}C$ macroalgal variations were analyzed in a large stock of specimens that vary in taxa and morphology and were collected in shallow marine habitats in the Gulf of California (GC) with distinctive environmental conditions. A large $\delta^{13}C$ variability (-34.6 ‰ to -2.2 ‰) was observed. Life-forms (taxonomy 57 %, morphology and structural organization 34 %) explain the variability related to carbon use physiology. Environmental conditions influenced the $\delta^{13}C$ macroalgal values but did not change the physiology, which is most likely inherently species-specific. Values of $\delta^{13}C$ were used as indicators of the presence or absence of carbon concentrating mechanisms (CCMs) and as integrative values of the isotope discrimination during carbon assimilation in the life cycle macroalgae. Based on $\delta^{13}C$ signals, macroalgae were classified in three strategies relative to the capacity of CCM: (1) HCO_3^- uptake ($\delta^{13}C > -10$ ‰), (2) using a mix of CO_2 and HCO_3^- uptake ($-10 < \delta^{13}C > -30$ ‰), and (3) CO_2 diffusive entry ($\delta^{13}C < -30$ ‰). Most species showed a $\delta^{13}C$ that indicates a CCM using a mix of CO_2 and HCO_3^- uptake. HCO_3^- uptake is also widespread among GC macroalgae, with many Ochrophyta species. Few species belonging to Rhodophyta relied on CO_2 diffusive entry exclusively, while calcifying macroalgae species using HCO_3^- included only *Amphiroa* and *Jania*. The isotopic signature evidenced the activity of CCM, but it was inconclusive about the preferential uptake of HCO_3^- and CO_2 in photosynthesis and the CCM type expressed in macroalgae. In the study of carbon use strategies, diverse, species-specific, and complementary techniques to the isotopic tools are required.

1 Introduction

Macroalgae show a wide diversity of thallus morphologies (e.g., filamentous, articulated, flattened), structural organization (e.g., surface area : volume ratio), and various photosynthetic pigments (e.g., Chlorophyll *a*, *b*, phycocyanin) (Lobban and Harrison, 1994). According to the predominant pigment contents in the thallus, macroalgae are classified into three phyla. The interaction of morphologies and photosynthetic pigments is classified into dozens of groups (Balata et al., 2011; Littler and Littler, 1980; Littler and Arnold, 1982). For example, the mixture of chlorophyll (*a*, *b*) and carotenoids is dominant in Chlorophyta, and chlorophyll (*a*, *c*) and fucoxanthin carotenoid are dominant in Ochrophyta, while Rhodophyta contains chlorophyll (*a*, *d*), carotenoid, and a mixture of phycobilin (e.g., phycocyanin, phycoerythrin, allophycocyanin) (Bold and Wynne, 1978; Gateau et al., 2017; Masojidek et al., 2004). Both traits work as an excellent approximation to explain the fundamentals of metabolism, growth, zonation, and colonization (Littler and

Littler, 1980; Littler and Arnold, 1982; Nielsen and Sand-Jensen, 1990; Vásquez-Elizondo and Enríquez, 2017).

In marine environments, where pH $\sim 8.1 \pm 1$, the diffusion rate of CO_2 in seawater is low. Thus, HCO_3^- accounts for 98 % of the total dissolved inorganic carbon (DIC), resulting in a high $HCO_3^- : CO_2$ ratio (150 : 1) (Sand-Jensen and Gordon, 1984). Low CO_2 concentrations in seawater, which limit macroalgae growth, are compensated for by carbon concentrating mechanisms (CCMs) that increase the internal inorganic carbon concentration near the site of RuBisCo activity (Giordano et al., 2005). Therefore, the absorption of HCO_3^- by most macroalgae is the primary source of inorganic carbon for photosynthesis, but some species depend exclusively on the use of dissolved CO_2 that enters cells by diffusion (Beardall and Giordano, 2002; Giordano et al., 2005; Maberly et al., 1992; Raven et al., 2002a, b). Hence, macroalgal species with productivity limited by lacking CCMs (having low plasticity for inorganic carbon uptake) seems to be restricted to subtidal habitats and composed mainly of red macroalgae (but without a morphological patron apparent) (Cornwall et al., 2015; Kübler and Dudgeon, 2015). The rest of the macroalgae with CCM occupies the intertidal to the deep subtidal zone.

The habitat features and environmental conditions in marine ecosystems modify the main macroalgae photosynthesis drivers, such as light (Anthony et al., 2004; Johansson and Snoeijs, 2002), DIC (Brodeur et al., 2019; Zeebe and Wolf-Gladrow, 2001), and inorganic nutrients (Ochoa-Izaguirre and Soto-Jiménez, 2015; Teichberg et al., 2010). These factors could generate negative consequences for their productivity, principally when they cause resource limitation. Each factor varies from habitat to habitat (e.g., local scale: from intertidal to subtidal zone; and global scale: from temperate to tropical regions), and in response to these environmental changes, macroalgae can modulate their photosynthetic mechanism (Dudgeon et al., 1990; Kübler and Davison, 1993; Lapointe and Duke, 1984; Young and Beardall, 2005). The modulation, to increase their photosynthetic activity (up-and-down regulation processes), implies a physiological acclimation enhancing the transport of DIC (CO_2, HCO_3^-) into the cell and its fixation rates (Enríquez and Rodríguez-Román, 2006; Giordano et al., 2005; Klenell et al., 2004; Madsen and Maberly, 2003; Rautenberger et al., 2015; Zou et al., 2004).

The δ^{13}C macroalgal values indicate the carbon source used (CO_2 or HCO_3^-) in photosynthesis and allow the presence or absence of CCMs to be inferred (Giordano et al., 2005; Maberly et al., 1992; Raven et al., 2002a). However, the isotopic signature may be inconclusive for determining the carbon source's preference (Roleda and Hurd, 2012). Also, the δ^{13}C signal in the algal thallus can be used to indicate the physiological state of photosynthetic metabolism (Kim et al., 2014; Kübler and Dungeon, 2015). For example, δ^{13}C variability depends, in part, on the life-forms' taxonomy, morphology, and structural organization (Lovelock et al., 2020; Marconi et al., 2011; Mercado et al., 2009; Roleda and Hurd, 2012). δ^{13}C is also modulated by the interaction with environmental conditions (e.g., light, DIC, and nutrients) (Carvalho et al., 2010a, b; Cornelisen et al., 2007; Dudley et al., 2010; Mackey et al., 2015; Rautenberger et al., 2015; Roleda and Hurd, 2012). In this study, our objective was to investigate the contributions of life-forms, the changes in the habitat features, and environmental conditions to the δ^{13}C macroalgal variability in communities in the Gulf of California (GC). We collected a large stock of macroalgae specimens of a diversity of species characterized by various morphological and physiological properties to reach our objective. Besides high diversity, in terms of life-forms, we selected various shallow marine habitats along a latitudinal gradient in the GC or the sample collection, characterized by unique and changing environmental factors. The GC features abundant and diverse macroalgae populations, acclimated and adapted to diverse habitats with environmental conditions determining the light, DIC, and nutrient availability. The δ^{13}C signal from the thallus of macroalgae was used as indicative of the presence or absence of CCMs and as integrative values of the isotope discrimination during carbon assimilation and respiration along the life cycle of macroalgae in macroalgal communities in the GC as a function of taxa and environmental factors (Díaz-Pulido et al., 2016; Hepburn et al., 2011; Maberly et al., 1992; Raven et al., 2002a). Because the GC is a subtropical zone with high irradiance and specimens were collected in the intertidal and shallow subtidal zone, we expect to find a high proportion of species with active uptake HCO_3^- ($\delta^{13}C > -10$ ‰). A third objective was to explore any geographical pattern in the δ^{13}C macroalgae along and between the GC bioregions. Previous studies have indicated changes in the δ^{13}C signal with latitude, mainly related to the light and temperature (Hofmann and Heesch, 2018; Lovelock et al., 2020; Marconi et al., 2011; Mercado et al., 2009; Stepien, 2015). Macroalgae as biomonitors constitute an efficient tool in monitoring programs in large geographical regions (Balata et al., 2011) and for environmental impact assessments (Ochoa-Izaguirre and Soto-Jiménez, 2015).

2 Materials and methods

2.1 Gulf of California description

The Gulf of California is a subtropical, semi-enclosed sea of the Pacific coast of Mexico, with exceptionally high productivity making it the most important fishing region for Mexico and one of the most biologically diverse worldwide marine areas (Espinosa-Carreón and Valdez-Holguín, 2007; Lluch-Cota et al., 2007; Páez-Osuna et al., 2017; Zeitzschel, 1969). The Gulf of California represents only 0.008 % of the area covered by the seas of the planet (265 894 km^2, 150 km wide, and 1000 km long covering $> 9^\circ$ latitude). However, the GC

has a high physiographic diversity and is biologically megadiverse with many endemic species, including ∼ 766 macrofauna species and/or subspecies in which the major number belong to Arthropoda (118 species) and Mollusca (460 species) taxa (Brusca et al., 2005; Espinosa-Carreón and Escobedo-Urías, 2017; Wilkinson et al., 2009) and 116 to macroalgae species (Espinoza-Avalos, 1993; Norris, 1975, 1985).

Regionalization criteria of the GC include phytoplankton distribution (Gilbert and Allen, 1943), topography (Rusnak et al., 1964) and depth (Álvarez-Borrego, 1983), oceanographic characteristics (Álvarez-Borrego, 1983; Marinone and Lavín, 2003; Roden and Emilson, 1979), biogeography (Santamaría-del-Ángel et al., 1994), and bio-optical characteristics (Bastidas-Salamanca et al., 2014). The topography is variable along the GC and includes submarine canyons, basins, and variable continental platforms. Besides, the GC presents complex hydrodynamic processes, including internal waves, fronts, upwelling, vortices, and mixing of tides. The gulf's coastline is divided into three shores: extensive rocky shores, long sandy beaches, numerous scattered estuaries, coastal lagoons, open muddy bays, tidal flats, and coastal wetlands (Lluch-Cota et al., 2007).

The Gulf of California is different in the north and the south, related to a wide range of physicochemical factors. The surface currents seasonally change direction and flow to the southeast with maximum intensity during the winter and to the northwest in summer (Roden, 1958). The northern part is very shallow (< 200 m deep on average), divided into the upper gulf, northern gulf, and Midriff Islands regions (Roden, 1958; Roden and Groves, 1959). The surrounding deserts largely influence this region (Norris, 2010), which shows marked seasonal changes in coastal surface seawater temperatures (Marinone, 2007; Martínez-Díaz-de-León et al., 2006). Tidal currents induce a significant cyclonic circulation through June to September and anticyclonic from November to April (Bray, 1988; Carrillo and Palacios-Hernández, 2002; Martínez-Díaz-de-León, 2001; Velasco-Fuentes and Marinone, 1999). The southern part consists of a series of basins whose depths increase southwards (Fig. 1). The intertidal macroalgae in the southern region are subject to desiccation, mostly during summer. The water column's physicochemical characteristics are highly influenced by the contrasting climatic seasons in the GC: the dry season (nominally from November to May) and the rainy season (from June to October). Annual precipitation ($1080\,mm\,yr^{-1}$) and evaporation ($56\,mm\,yr^{-1}$) rates registered during the past 40 years were $881 \pm 365\,mm\,yr^{-1}$ and $53 \pm 7\,mm\,yr^{-1}$, respectively (CNA, 2012).

In the GC around 669 macroalgae species exist, including 116 endemic species (Espinoza-Avalos, 1993; Norris, 1975; Pedroche and Sentíes, 2003). Many endemic species currently have a wide distribution along the Pacific Ocean coast but with GC origin (Aguilar-Rosas et al., 2014; Dreckman, 2002). Based on oceanographic characteristics (Roden and Groves, 1959) and in the endemic species distribution (Aguilar-Rosas and Aguilar-Rosas, 1993; Avalos, 1993), the GC can be classified into three phycofloristic zones: (1) the first zone located from the imaginary line connecting San Francisquito Bay, B.C. (Baja California), to Guaymas, Sonora, with 51 endemic species; (2) the second zone with an imaginary line from La Paz Bay (B.C.S.; Baja California Sur) to Topolobampo (Sinaloa) with 41 endemic species; (3) the third zone is located with an imaginary line from Cabo San Lucas (B.C.S.) to Cabo Corrientes (Jalisco) with 10 endemic species. Besides, 14 endemic species are distributed throughout the GC (Espinoza-Ávalos, 1993). The macroalgal communities are subject to the changing environmental conditions in the diverse habitats in the GC that delimit their zonation, which tolerates a series of anatomical and physiological adaptations to water movement, temperature, sun exposure, light intensities, low pCO_2, and desiccation (Espinoza-Avalos, 1993).

2.2 Macroalgae sampling

In this study, the GC coastline (21–30° N latitude) was divided into six coastal sectors based on the three phycofloristic zones along peninsular and continental GC coastlines (Fig. 1a). In each coastal sector, selected ecosystems and representative habitats were sampled based on macroalgae communities' presence and habitat characterization. Habitats were classified by substrate type (e.g., sandy-rock, rocky shore), hydrodynamic (slow to faster water flows), protection level (exposed or protected sites), and immersion level (intertidal or subtidal) (Fig. 1b).

Based on the local environmental factors, four to five macroalgae specimens of the most representative species were gathered by hand (free diving) during low tide. A total of 809 composite samples were collected from marine habitats along both GC coastlines. The percentages of specimens collected for the substrate type were 28 % sandy-rock and 72 % rocky shores based on the habitat features. In the hydrodynamic, 30 % of the specimens were collected in habitats with slow to moderate and 70 % with moderate to fast water movement. Regarding the protection level, 57 % were exposed specimens, and 43 % were protected. Finally, 56 % were intertidal and 44 % subtidal macroalgae organisms concerning the emersion level. About half of the protected specimens were collected in isolated rock pools, which was noted.

In four to five sites of each habitat, we measured in situ the salinity, temperature, and pH by using a calibrated multiparameter sonde (Y.S.I. 6600V) and the habitat characteristics mentioned above noted. Besides, composite water samples were collected for a complementary analysis of nutrients, alkalinity (and their chemical components), and $\delta^{13}C$ DIC (data not included). Briefly, the representative habitats were classified by pH levels of > 9.0 "alkalinized", 7.9–8.2 "typical", and < 7.9 "acidified". Based on colder (< 20 °C), typical (20–25 °C), and warmer (> 25 °C) temperatures, 72 % of

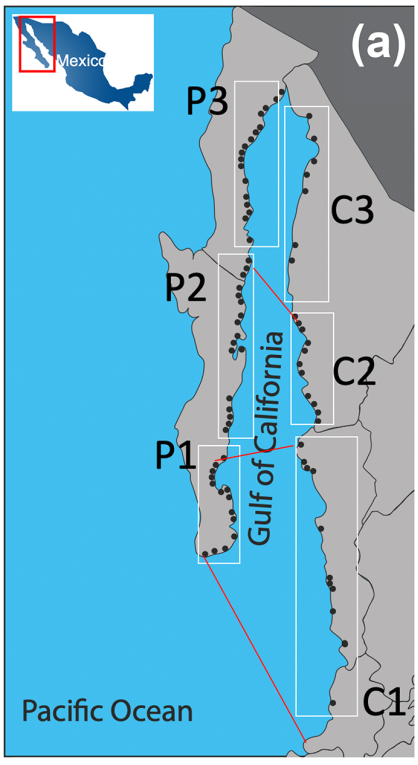

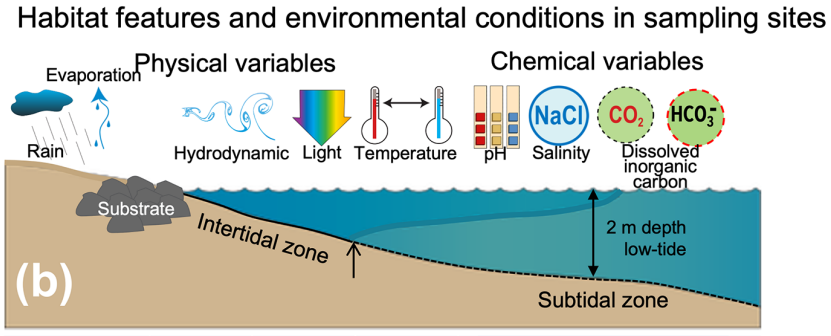

Environmental factors	Continental GC coastline			Peninsula GC coastline		
	C1	C2	C3	P1	P2	P3
Substrate at shores	Rocky and sandy-rocky	Only sandy-rocky shore	Rocky and sandy-rocky	Rocky and sandy-rocky	Rocky and sandy-rocky	Rocky and sandy-rocky
Hydrodynamic (water movement)	Slow to fast	Slow to fast	Slow to fast	Slow to fast	Slow to fast	Slow to fast
Protection level sites	Exposed and protected	Exposed and protected	Exposed and protected	Exposed and protected	Exposed and protected	Exposed and protected
Immersion level	Intertidal and subtidal	Intertidal and subtidal	Intertidal and subtidal	Intertidal and subtidal	Intertidal and subtidal	Intertidal and subtidal
pH ranges	Acid, typical and alkaline	Acid, typical and alkaline	Acid, typical and alkaline	Acid, typical and alkaline	Typical and alkaline	Acid, typical and alkaline
Temperature ranges	Typical and warmer	Colder, typical and warmer	Colder, typical and warmer	Colder, typical and warmer	Colder, typical and warmer	Colder, typical and warmer
Salinity ranges	Marine	Hypersaline, marine, estuarine	Marine	Marine	Marine	Marine

Figure 1. Site collection along the continental (C1–C3) and peninsular (P1–P3) Gulf of California coastlines **(a)**, range of environmental factors supporting or limiting the life processes for the macroalgal communities within a habitat **(b)**, and inserted table with the features and environmental conditions in the diverse habitats in the GC bioregions that delimit the macroalgal community's zonation.

the specimens were collected at typical, 22 % at alkalinized, and 6 % at acidified pH values. Regarding the temperature, about 55 % of the specimens were collected at typical, 31 % at warmer, and 14 % at colder seawaters. Regarding salinity, most of the ecosystems showed typical values for seawater (35.4 ± 0.91 PSU, from 34.5 to 36.1 PSU). In this study, the collection surveys were conducted during spring (March–April) and dry season (nominally from November to May) from 2008 to 2014. Only in a few selected ecosystems located at C1, C2, and C3 sectors was one sampling survey conducted at the end of the rainy season (nominally from June to October in 2014). Thus, these ecosystems were possible to include habitat with a salinity range varying from estuarine (23.5 ± 3.0 PSU) to hypersaline (42.7 ± 7.0 PSU) values. These habitats were mainly isolated rock pools, and only a few were sites near tidal channels receiving freshwater discharges. About 95 % of the specimens were collected at typical seawater salinity (34–36 PSU) and only 1.5 % and 3.5 % in estuarine (< 30 PSU) and hypersaline (> 37 PSU) environments, respectively. Detailed information on the selected shallow marine ecosystems, habitat characterization, and environmental conditions is summarized in the inserted table in Fig. 1.

2.3 Macroalgae processing and analysis of the isotopic composition of carbon

The collected material was washed in situ with surface seawater to remove the visible epiphytic organisms, sediments, sand, and debris and then thoroughly rinsed with Milli-Q water. The composite samples were double-packed in a plastic bag, labeled with the locality's name and collection date, placed in an ice cooler to be kept to 4 °C, and immediately transported to the laboratory UAS-Facimar in Mazatlán. In the field, sample aliquots were also preserved in 4 % v/v formaldehyde solution for taxonomic identification to the genus or species level (when possible). The following GC macroalgal flora identification manuals were consulted (Abbot and Hollenberg, 1976; Dawson, 1944, 1954, 1956, 1961, 1962, 1963; Norris, 2010; Ochoa-Izaguirre et al., 2007; Setchell and Gardner, 1920, 1924).

In the laboratory, macroalgae samples were immediately frozen at −30 °C until analysis. Then, samples were freeze-dried at −38 °C and 40 mm Hg for 3 d, upon which they were ground to a fine powder and exposed to HCl vapor for 4 h (acid-fuming) to remove carbonates and dried at 60 °C for 6 h (Harris et al., 2001). Aliquots of ∼ 5 mg were encapsulated in tin cups (5 × 9 mm) and stored in sample trays until analysis. Macroalgae samples were sent to the Sta-

ble Isotope Facility (SIF) at the University of California at Davis, CA, USA. Natural ^{13}C relative abundance relative to ^{12}C in samples was determined with mass spectrometry, using a Carlo Erba elemental analyzer attached to a Finnigan Delta S mass spectrometer equipped with a Europa Scientific stable isotope analyzer (ANCA-NT 20-20) and a liquid–solid preparation unit (PDZ, Europa, Crewz, UK). Isotope ratios of the samples were calculated using the equation δ (‰) $= [(R_{\text{sample}}/R_{\text{standard}} - 1) \times 1000]$, where $R = {}^{13}\text{C}/{}^{12}\text{C}$. The R_{standard} is relative to the international V-PDB (Vienna PeeDee Belemnite) standard. During the isotopic analysis, the SIF lab used different certified reference materials (e.g., IAEA-600, USGS-40, USGS-41, USGS-42, USGS-43, USGS-61, USGS-64, and USGS-65) for the analytical control quality. The analytical uncertainties reported for the SIF lab were 0.2 ‰ for δ^{13}C (https://stableisotopefacility.ucdavis.edu/carbon-and-nitrogen-solids, last access: 18 January 2021). We also included triplicate aliquots of several specimens of the same species and condition, collected from one patch or attached to the same substrate, to assess the method error by sampling and processing procedures. The methodological uncertainties were < 0.4 ‰.

2.4 Analysis of δ^{13}C macroalgal variability

The variability in δ^{13}C values in macroalgae was analyzed as a function of the taxonomy (phylum, genus, and species) and morphofunctional groups (e.g., thallus structure, growth form, branching pattern, and taxonomic affinities; Balata et al., 2011; Ochoa-Izaguirre and Soto-Jiménez, 2015). The carbon fixation strategies in the macroalgae communities of the GC were identified by δ^{13}C (Díaz-Pulido et al., 2016; Hepburn et al., 2011) in agreement with the Maberly et al. (1992) and Raven et al. (2002a) thresholds. So, macroalgae were classified into three strategies for DIC uptake: (1) CCM only by active uptake HCO_3^- ($\delta^{13}\text{C} > -10$ ‰), (2) CCM active uptake HCO_3^- and diffusive uptake CO_2 ($\delta^{13}\text{C} < -11$ to -30 ‰), and (3) non-CCM CO_2 by diffusion only ($\delta^{13}\text{C} < -30$ ‰). The measured δ^{13}C macroalgal signals are integrative of the discrimination by photosynthesis ($\Delta^{13}\text{C}_\text{p}$) on the carbon source ($\delta^{13}$C DIC in seawater), respiration ($\Delta^{13}\text{C}_\text{r}$), and probable CO_2 leak out inside the cell during the CCM process (Carvalho et al., 2009a, b; Raven et al., 2005; Sharkey and Berry, 1985).

Macroalgae were grouped according to their morphofunctional characteristics proposed initially by Littler and Littler (1980) and modified by Balata et al. (2011). Most of the macroalgae species showed a limited distribution along the GC coastlines. Few cosmopolites' species included *Colpomenia tuberculata*, *Sargassum sinicola*, *Padina durvillei*, and *Ulva lactuca*. Also, not all morphofunctional groups and taxa were present in every site during each sampling survey, and the sample size in each group varied for taxa, location, and time.

A basic statistical analysis of δ^{13}C values in different macroalgae groups was applied to distribute and calculate the arithmetic mean, standard deviation, and minimum and maximum. Because not all macroalgal species were present in sufficient numbers at different collection habitats, several macroalgal groups were not considered for statistical analysis. We compared taxa and morphofunctional groups collected in the same habitat (within-subjects factor) by multivariate analysis of variance. When differences were noted, a Tukey–Kramer HSD (honestly significant difference) test was performed. Besides, variations in δ^{13}C macroalgae in specimens of the same morphofunction and taxon collected in different habitats were also investigated with a Kruskal–Wallis test.

The relationships between δ^{13}C with the inherent macroalgae properties (taxon and morphology), biogeographical collection zone (GC coastline and coastal sector), habitat features (substrate, hydrodynamic, protection, and emersion level), and environmental conditions (temperature, pH, and salinity) were examined through simple and multiple linear regression analyses. Excepting temperature, pH, and salinity, most of the independent variables are categorical independent variables. Simple linear regression analyses were performed to establish the relationships between δ^{13}C macroalgae with each environmental parameter analyzed as possible driving factors (e.g., temperature, salinity, and pH). Multiple linear regression analyses were conducted to evaluate the combined effects of those independent variables (macroalgae properties, biogeographical collection zone, habitat features, and environmental conditions) on the δ^{13}C macroalgae. In the multivariable regression model, the dependent variable, δ^{13}C macroalgal values, is described as a linear function of the independent variables X_i, as follows:

$$\delta^{13}\text{C-macroalgal} = a + b_1(X_1) + b_2(X_2) + \ldots + b_n(X_n), \quad (1)$$

where a is regression constant (it is the value of intercept, and its value is zero), b_1, b_2, and b_n are regression coefficients for each independent variable X_i. From each one of the fitted regression models, we extracted the estimated regression coefficients for each of the predictor variables: e.g., Bayesian information criterion (BIC), Akaike information criterion (AIC), root-mean-square error (RMSE), Mallow's Cp criterion, F ratio test, the p value for the test (prob $> F$), coefficients of determination (R^2), and the adjusted R^2 statistics (Stroup et al., 2018). All regression coefficients were used as indicators of the quality of the regression (Burnham and Anderson, 2002; Draper and Smith, 1998). The Kolmogorov–Smirnov normality test was applied for all variables, and all were normally distributed. Most of the δ^{13}C values in each group showed a normal distribution. For all statistical tests, a probability $P < 0.05$ was used to determine statistical significance. The statistical analysis of the results was using JMP 14.0 software (SAS Institute Inc.).

3 Results

3.1 Taxonomy and morphofunctional groups

Sampled specimens belong to 3 phyla, 63 genera, and 170 species. The phyla were identified as Chlorophyta (25 %), Ochrophyta (22 %), and Rhodophyta (53 %). The most representative genera (and their species) were *Ulva* (*U. lactuca, U. lobata, U. flexuosa*, and *U. intestinalis*), *Codium* (*C. amplivesiculatum* and *C. simulans*), *Chaetomorpha* (*C. antennina*), *Padina* (*P. durvillei*), *Dictyota* (*D. dichotoma*), *Colpomenia* (*C. tuberculata* and *C. sinuosa*), *Sargassum* (*S. sinicola* and *S. horridum*), *Amphiroa* (*Amphiroa* spp.), *Spyridia* spp., *Polysiphonia* spp., *Gymnogongrus* spp., *Gracilaria* (*G. vermiculophylla, G. pacifica*, and *G. crispata*), *Hypnea* (*H. pannosa* and *H. johnstonii*), *Grateloupia* (*G. filicina* and *G. versicolor*), and *Laurencia* (*L. papillosa* and *L. pacifica*). The endemic species included Chlorophyta *Codium amplivesiculatum*, Rhodophyta *Laurencia papillosa*, *Chondracanthus squarrulosa*, *Gracilaria spinigera*, and *G. subsecundata*, and Ochrophyta *Cutleria hancockii, Sargassum herphorizum*, and *S. johnstonii*.

An analysis of the biogeographical diversity among sectors evidenced that P3 (43 genera of 63, 68 %) and C3 (63 %) in the north recorded the highest number of the genus, followed by C1 (38 %) and P1 (29 %) in the south, and P2 (27 %) and C2 (22 %). The same pattern was observed in the species diversity: zones P3 (94 of 167 species, 56 %) and C3 (52 %) in the north, C1 (34 %) and P1 (25 %) in the south, and C2 and P2 (19 %–20 %) in the center.

The morphofunctional groups identified were 21. The most common were C-Tubular (6 species, $n = 69$); C-Blade-like (6 species, $n = 55$); C-Filamentous uniseriate (17 species, $n = 49$); C-Erect thallus (5 species, $n = 33$); O-Compressed with branched or divided thallus (19 species, $n = 92$); O-Thick leathery macrophytes (12 species, $n = 104$); O-Hollow with spherical or subspherical shape (4 species, $n = 87$); R-Larger-sized corticated (57 species, $n = 225$); R-Filamentous uniseriate and pluriseriate with erect thallus (9 species, $n = 48$); and R-Larger-sized articulated corallines (6 species, $n = 17$). The diversity, in terms of presence/absence of the morphofunctional groups, varied among coastline sectors and was higher in C3 (16 of 21, 76 %) and P3 (71 %) in the north, followed by C1 (57 %) and P1 (48 %) in the south, and C2 and P2 and (42 %–48 %) in the center of both GC coastlines.

3.2 The δ^{13}C macroalgal variability as a function of taxonomic and morphofunctional groups

The variability in δ^{13}C values in macroalgae was analyzed by taxon (phylum, genus, species) and morphofunctional groups classified by habitat, coastal sector, and collection season. A complete list of the results of δ^{13}C in 170 macroalgae species is provided in Supplement (Table S1). Firstly, δ^{13}C values analyzed by phylum showed a unimodal distribution with a peak at -14 ± 1.4 ‰ (Fig. 2). Ochrophyta (-21.5 ‰ to -2.2 ‰, -12.5 ± 3.7 ‰), displayed significantly higher values than Chlorophyta (-25.9 ‰ to -5.5 ‰, -14.5 ± 3.0 ‰) and Rhodophyta (-34.6 ‰ to -4.5 ‰, -14.8 ± 3.9 ‰). The δ^{13}C macroalgal values (average $\pm$ SD) for the genera of Chlorophyta, Ochrophyta, and Rhodophyta (Fig. 3) varied from -33.8 ± 1.1 ‰ for *Schizymenia* to -7.8 ± 0.7 ‰ for *Amphiroa*. Based on the highest values, specimens of three phyla showed δ^{13}C values > -10 ‰, which evidenced the presence of CCMs by active uptake of HCO_3^- (strategy 1) (Fig. 3). For example, *Caulerpa, Cladophora, Codium*, and *Ulva* for Chlorophyta, *Colpomenia, Dictyota, Padina*, and *Sargassum* for Ochrophyta, and *Hypnea* and *Polysiphonia* for Rhodophyta showed δ^{13}C values > -10 ‰. Likewise, high δ^{13}C values were observed in the calcifying macroalgal genera *Amphiroa* and *Jania* under strategy 1 (Fig. 3c). The δ^{13}C values lower than -30 ‰ that denote uptake of CO_2 by diffusion (strategy 3) were observed only in Rhodophyta *Schizymenia*, *Halymenia*, and *Gigartina*. However, most species showed large δ^{13}C variabilities, which is evidence of a mechanism that uses a mix of HCO_3^- and CO_2 for photosynthesis (strategy 2).

Multiple comparison analyses revealed significant differences in the δ^{13}C macroalgal values among genera, ordered as *Schizymenia* < *Polysiphonia* < *Ulva*, *Gracilaria* and *Spyridia* (-16.1 ± 0.6 ‰ to -15.1 ± 0.2 ‰) < *Gymnogongrus, Laurencia, Hypnea, Cladophora, Dictyota, Sargasum, Chaetomorpha*, and *Grateloupia* (from -15.4 ± 0.7 ‰ to -13.8 ± 0.8 ‰) < *Codium* and *Padina* (-12.5 ± 2.4 ‰ to -12.4 ± 2.5 ‰) < *Colpomenia* and *Amphiroa* (-9.2 ± 0.3 ‰ to -7.8 ± 0.7 ‰) ($F = 16.81$, $p < 0.001$).

Aggrupation of δ^{13}C values based on morphofunctional features is displayed in Fig. 4. The most representative groups in the phylum Chlorophyta varied from -15.8 ± 0.3 ‰ for C-Tubular to -12.4 ± 0.5 ‰ for C-Thallus erect. The phylum Ochrophyta includes O-Thick leathery with the lowest mean (-14.8 ± 0.3 ‰) and O-Hollow with a spherical or subspherical shape with the highest values (-9.2 ± 0.3 ‰). The lowest and highest δ^{13}C values for Rhodophyta were observed for R-flattened macrophytes (-24.0 ± 9.6 ‰) and R-Larger-sized articulated coralline (-7.9 ± 0.8 ‰), respectively. Significant differences were observed among groups, which were ordered as follows: R-Flattened macrophytes < R-Blade-like < C-Tubular < O-Tick leathery and R-Larger-sized corticated < C-Blade-like and C-Filamentous uniseriate < C-Thallus erect and O-Compressed with branch < O-Hollow with spherical < R-Larger-sized articulated coralline.

High intraspecific variability in δ^{13}C signal for the more representative genera of each taxon is showed in Tables 1–3. For *Codium*, *C. brandegeei* (11.8 ± 1.2 ‰) and *C. simulans* (-11.4 ± 2.2 ‰) showed higher δ^{13}C values than *C. amplivesculatum* (-14.4 ± 2.7 ‰). *Colpomenia* species

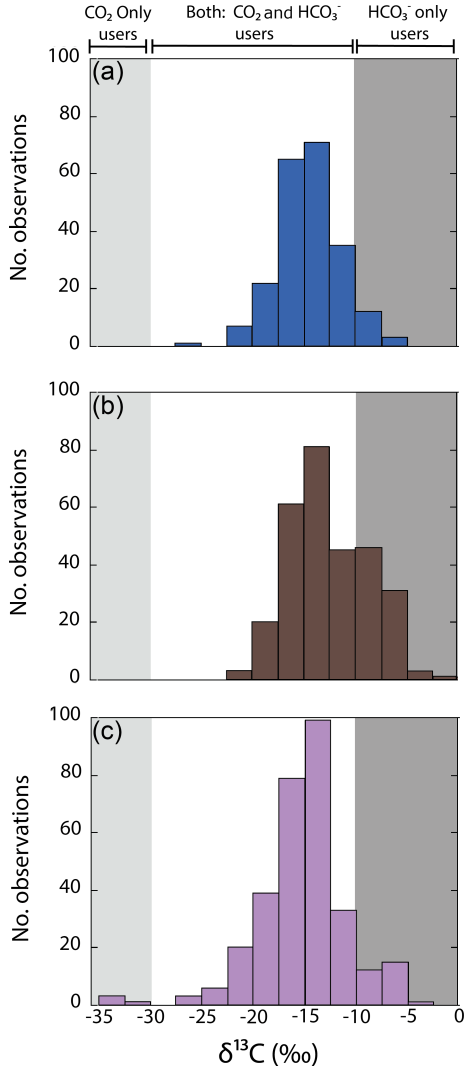

Figure 2. Variability in δ^{13}C values for specimens of different macroalgae species collected along GC coastlines classified by taxon: **(a)** Chlorophyta, **(b)** Ochrophyta, and **(c)** Rhodophyta. Shaded background represents the cutoff limits for using CO_2 only users and HCO_3^- only users, according to Raven et al. (2002a).

had higher δ^{13}C values than the other genera, with higher values for *C. tuberculata* (-8.7 ± 3.2 ‰) than *Colpomenia* sp. (-10.9 ± 3.6 ‰) and *C. sinuosa* (-10.2 ± 2.9 ‰). *Gracilaria* showed comparable δ^{13}C values in the four species (from -16.4 ± 1.6 ‰ for *G. pacifica* to -15.5 ± 2.4 ‰ for *Gracilaria* sp.). *Hypnea* showed non-significant δ^{13}C differences in three representative species (-16.4 ± 1.7 ‰ for *H. spinella* to -14.9 ± 2.3 ‰ for *Hypnea* sp.). *Laurencia* sp. (-12.9 ± 1.2 ‰) was higher than *L. pacifica* (-14.9 ± 2.2 ‰), while *Padina* sp. (-11.1 ± 1.5 ‰) higher than *P. durvillei* (-13.2 ± 2.6 ‰). *Sargassum* was one of the most diverse genera studied with six representative species, with δ^{13}C values ordered as follow: *S. horridum* = *S. sinicola* = *S. johnstonii* (-15.5 ± 2.9 to -15.1 ± 2.4 ‰) < *S. lapazeanum* (-14.5 ± 1.6 ‰) = *Sargassum* sp. (-14.2 ± 2.3 ‰) < *S. herphorizum* (-13.6 ± 1.6 ‰). *Spyridia* sp. (-17.0 ± 1.2 ‰) and *S. filamentosa* (-15.8 ± 3.8 ‰) showed non-significant differences. The six representative species of *Ulva* were divided into two morphological groups, filamentous and laminates. Filamentous species averaged -16.3 ± 2.0 ‰ for *U. clathrata*, -16.0 ± 3.6 ‰ for *U. flexuosa*, -15.7 ± 1.7 ‰ for *U. acanthophora*, and -15.3 ± 2.5 ‰ for *U. intestinalis*, and *Ulva* laminates included *U. linza* (-15.5 ± 2.4 ‰) and *U. lactuca* (-14.1 ± 3.1 ‰). Non-significant differences were observed between morphological groups and among species. A high intra-specific variability, 11 %–28 %, explains average overlapping.

Table 1. Carbon isotopic composition (‰) in species of phylum Chlorophyta collected along the Gulf of California coastlines.

Species (*n* composite samples)	δ^{13}C ± SD (min to max, ‰)
Chaetomorpha sp. (3)	-13.7 ± 0.8 (-14.6 to -12.9)
C. antennina (10)	-14.6 ± 1.1 (-16.3 to -12.8)
C. linum (5)	-16.8 ± 1.6 (-18.4 to -14.6)
Codium sp. (5)	-11.6 ± 3.0 (-14.1 to-6.7)
C. amplivesiculatum (8)	-14.4 ± 2.7 (-20.4 to -11.3)
C. brandegeei (7)	-11.8 ± 1.2 (-13.7 to -10.4)
C. fragile (4)	-13.0 ± 2.7 (-14.8 to -9.0)
C. simulans (9)	-11.4 ± 2.2 (-14.9 to -8.3)
Ulva sp. (12)	-14.0 ± 3.9 (-19.2 to -7.1)
U. acanthophora (25)	-15.8 ± 1.7 (-18.3 to -11.4)
U. clathrata (8)	-16.4 ± 2.0 (-20.5 to -14.5)
U. compressa (4)	-17.8 ± 2.4 (-20.6 to -15.4)
U. flexuosa (13)	-16.0 ± 3.7 (-25.9 to -10.4)
U. intestinalis (16)	-15.3 ± 2.5 (-20.3 to -8.9)
U. lactuca (31)	-14.1 ± 3.1 (-19.6 to -7.7)
U. linza (6)	-15.6 ± 2.4 (-19.4 to -13.2)
U. lobata (5)	-13.2 ± 1.9 (-15.3 to -11.1)
U. prolifera (3)	-14.2 ± 1.8 (-15.5 to -12.2)

3.3 δ^{13}C macroalgal variability in coastal sectors

A diversity of macroalgal assemblages were documented along the GC coastlines, with differences in the taxonomic composition according to their fico-floristic region. Multiple comparison analyses of δ^{13}C signals evidenced significant differences between the most common genera and species of macroalgae between and within assemblages grouped by coastal sector, season, and collecting year (Tables S2–S3). For example, genera *Padina* (e.g., *P. durvillei*) and *Ulva* (e.g., *U. lactuca*), collected in C1 sector during the rainy season, showed lower δ^{13}C values than in other sectors. Differences in the δ^{13}C signal are mainly related to the carbon uptake strategies of the macroalgae (Fig. 5). Even though most species inhabiting the GC coastal sectors dominated strategies based on active CCMs, the tendencies differed between taxa and coastal regions. Strategy 2 with mixing DIC sources

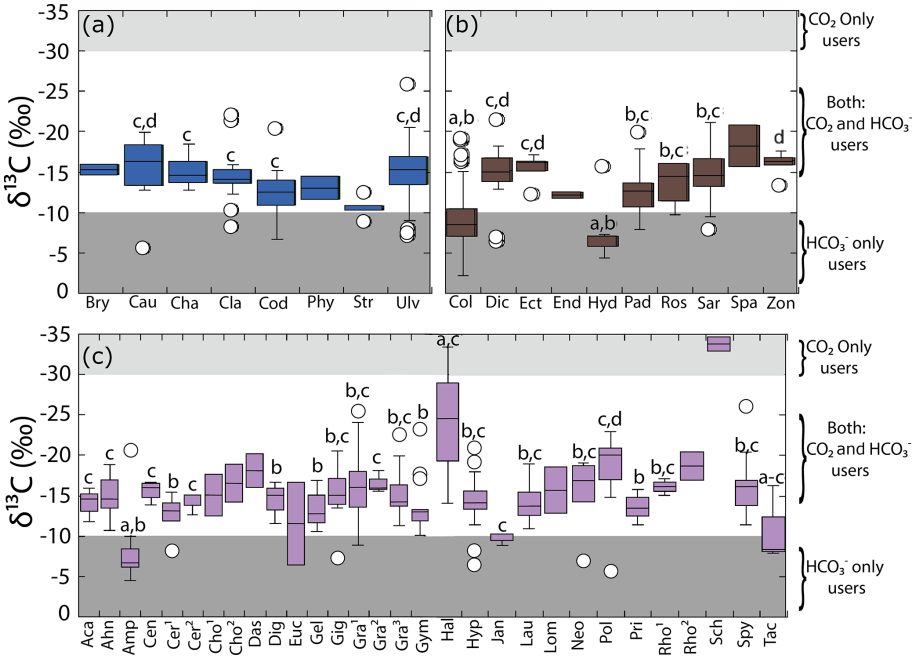

Figure 3. Variability in δ^{13}C values for the genera collected along the coastline of the Gulf of California according to their taxon: **(a)** Chlorophyta, **(b)** Ochrophyta, and **(c)** Rhodophyta. Genera with $n = 1$ are not shown, and genera with $n = 2$ were not considered in the statistical comparison. Different letters indicate significant differences ($P < 0.05$): $a > b > c > d > e$. Shaded background represents the cutoff limits for using CO_2 only users and HCO_3^- only users, according to Raven et al. (2002a). For Chlorophyta: Bry = Bryopsis, Cau = Caulerpa, Cha = Chaetomorpha, Cla = Cladophora, Cod = Codium, Phy = Phyllodictyon, Str = Struveopsis, Ulv = Ulva. Ochrophyta: Col = Colpomenia, Dic = Dictyota, Ect = Ectocarpus, End = Endarachne, Hyd = Hydroclathrus, Pad = Padina, Ros = Rosenvingea, Sar = Sargassum, Spa = Spatoglossum, Zon = Zonaria. Rhodophyta: Aca = Acantophora, Ahn = Ahnfeltiopsis, Amp = Amphiroa, Cen = Centroceras, Cer^1 = Ceramium, Cer^2 = Ceratodictyon, Cho^1 = Chondracanthus, Cho^2 = Chondria, Das = Dasya, Dig = Digenia, Euc = Eucheuma, Gel = Gelidium, Gig = Gigartina, Gra^1 = Gracilaria, Gra^2 = Grateloupia, Gra^3 = Gracilariopsis, Gym = Gymnogongrus, Hal = Halymenia, Hyp = Hypnea, Jan = Jania, Lau = Laurencia, Lom = Lomentaria, Neo = Neosiphonia, Pol = Polysiphonia, Pri = Prionitis, Rho^1 = Rhodoglossum, Rho^2 = Rhodymenia, Sch = Schizymenia, Spy = Spyridia, Tac = Tacanoosca.

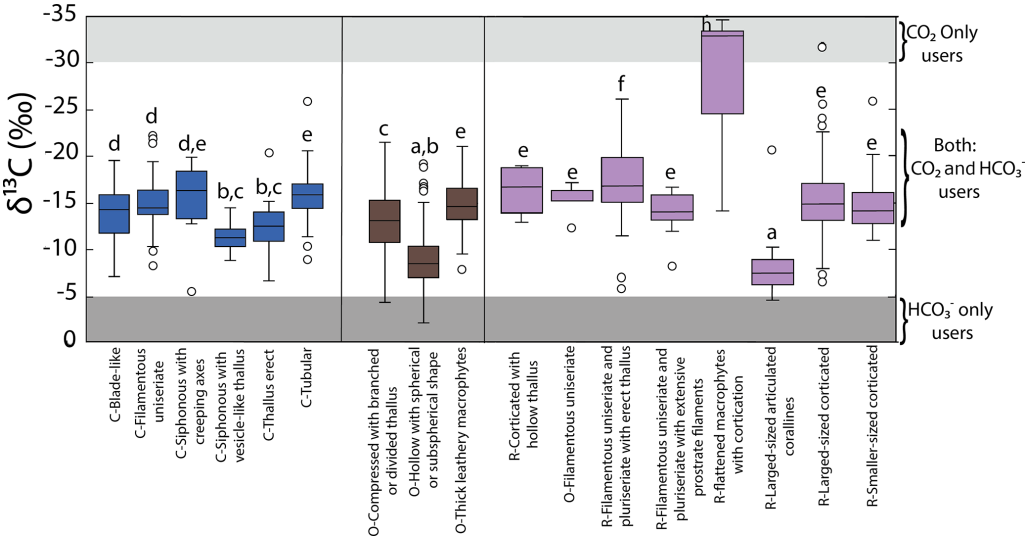

Figure 4. Variability in δ^{13}C values for morphofunctional groups by taxa along the coastline of the Gulf of California.

Table 2. Carbon isotopic composition (‰) in species of phylum Ochrophyta collected along the Gulf of California coastlines.

Species (*n* composite samples)	δ^{13}C ± SD (min to max, ‰)
Colpomenia sp. (11)	−11.0 ± 3.7 (−19.0 to −5.4)
C. ramosa (4)	−11.4 ± 2.6 (−13.8 to−7.8)
C. sinuosa (7)	−10.2 ± 3.0 (−16.3 to −7.2)
C. tuberculata (64)	−8.7 ± 3.2 (−19.2 to −2.2)
Padina sp. (15)	−11.1 ± 1.5 (−13.1 to−7.9)
P. crispata (3)	−11.3 ± 1.7 (−12.5 to −10.1)
P. durvillei (36)	−13.2 ± 2.6 (−20.0 to −9.2)
Sargassum sp. (34)	−14.3 ± 2.4 (−18.7 to −8.0)
S. herporhizum (7)	−13.7 ± 1.6 (−16.6 to −11.5)
S. horridum (12)	−15.5 ± 2.9 (−19.7 to−9.5)
S. johnstonii (10)	−15.4 ± 2.0 (−17.7 to −11.8)
S. lapazeanum (7)	−14.5 ± 1.6 (−17.2 to −12.8)
S. sinicola (31)	−15.1 ± 2.4 (−21.1 to −12.1)

Table 3. Carbon isotopic composition (‰) in species of phylum Rhodophyta collected along the Gulf of California coastlines.

Species (*n* composite samples)	δ^{13}C ± SD (min to max, ‰)
Gracilaria sp. (18)	−15.5 ± 2.4 (−21.8 to −12.2)
Gracilaria sp.2 (3)	−14.4 ± 3.7 (−18.7 to −12.3)
G. crispata (7)	−15.1 ± 3.0 (−19.1 to −10.1)
G. pacifica (6)	−16.5 ± 1.6 (−18.6 to −13.6)
G. spinigera (3)	−14.9 ± 3.8 (−17.7 to −12.2)
G. subsecundata (8)	−15.9 ± 2.8 (−20.3 to −12.8)
G. tepocensis (3)	−15.1 ± 1.9 (−17.0 to −13.2)
G. textorii (4)	−16.2 ± 2.6 (−18.1 to −14.3)
G. turgida (5)	−15.3 ± 3.6 (−20.7 to −12.0
G. vermiculophylla (16)	−15.9 ± 3.8 (−23.4 to −8.8)
Hypnea sp. (14)	−14.9 ± 2.6 (−20.9 to −11.4)
H. johnstonii (5)	−11.2 ± 3.5 (−13.8 to −6.5)
H. pannosa (5)	−11.8 ± 3.3 (−15.0 to −6.4)
H. spinella (6)	−16.4 ± 1.8 (−19.2 to −14.9)
H. valentiae (6)	−15.2 ± 2.3 (−19.2 to −12.7)
Laurencia sp. (8)	−12.9 ± 1.2 (−14.7 to −10.5)
L. pacifica (8)	−14.9 ± 2.2 (−19.0 to −12.7)
L. papillosa (3)	−15.7 ± 0.3 (−15.9 to −15.6)
Spyrida sp. (5)	−17.1 ± 1.12 (−19.1 to −16.1)
S. filamentosa (14)	−15.9 ± 3.8 (−26.2 to −11.5)

is dominant in all regions and taxa (60 %–90 %). Exceptions were observed in the P1 (68 %) and C1 (37 %) regions for Ochrophyta, in which the specialized strategy 1 (the HCO_3^- user) was significant. Strategy 3 based on the use of CO_2 was observed in the peninsular coast in P2 and P3 for Rhodophyta with 2 %–3.3 %. Overall, more negative δ^{13}C values were observed at continental (C2) compared to the peninsular coastline (P1–P3) and southward than northward.

3.4 The δ^{13}C macroalgal variability as a function of taxonomy, habitat features, and environmental conditions

Variability in δ^{13}C values for the most representative genera was evaluated by multiple comparative analyses as a function of habitat features, including the substrate, hydrodynamic, and emersion level. Large δ^{13}C variability observed between specimens of the same genus collected in the different habits do not show any significant pattern, and non-significant differences were observed. An exception was observed with the emersion level (shown in Fig. 6), in which intertidal specimens recorded less negative values than subtidal in most macroalgae genera, for example, for *Hydroclathrus* (intertidal −5.7 ± 0.9 ‰, subtidal −11.4 ± 5.9 ‰), *Amphiroa* (intertidal −6.9 ± 1.5, subtidal −9.9 ± 6.1 ‰), *Hypnea* (intertidal −13.5 ± 2.5 ‰, subtidal −18.6 ± 1.8 ‰), and *Laurencia* (intertidal −13.5 ± 1.3 ‰, subtidal −17.1 ± 1.8 ‰). Exceptions were observed for *Polysiphonia* (intertidal −19.7 ± 2.2 ‰, subtidal −14.9 ± 6.7 ‰), *Spyridia* (intertidal −16.9 ± 3.3 ‰, subtidal −13.2 ± 0.7 ‰), and *Colpomenia* (intertidal −9.4 ± 3.4 ‰, subtidal −7.7 ± 1.3 ‰).

Non-significant differences were observed for the same genera at different temperature ranges except for *Grateloupia* (cold, −19.2 ± 4.7 ‰, typical −14.4 ± 2.2 ‰, warm −14.5 ± 2.2 ‰) and *Polysiphonia* (cold, −21.0 ± 0.4 ‰, typical −18.1 ± 5.5 ‰, warm −17.9 ± 2.3 ‰) with more negative values in colder than warmer waters ($F = 6.42$, $p < 0.001$). Neither significant difference was observed in δ^{13}C values in macroalgae specimens from the different genera in the same temperature range (Fig. 7a).

Significant differences were observed among the genera related to the pH level in seawater (Fig. 7b). Under typical pH seawater, *Amphiroa* and *Colpomenia* were 1 ‰–2 ‰ more negatives than in alkaline waters, while *Ulva* and *Spyridia* were 3 ‰–5 ‰ less negative than in acidic waters. *Amphiroa* and *Colpomenia* were not collected in acidic water, and neither was *Spyridia* in alkaline waters to compare. Another genus also showed extremes values between alkaline (*Tacanoosca* −7.6 ± 1.0 ‰) and acidic waters (*Schizymenia* −32.9 ± 2.0 ‰). The following order was observed in the genera collected at the three pH ranges: alkaline > typical > acidic. Significant differences were observed for genera *Ahnfeltiopsis, Caulerpa, Gymnogongrus, Padina*, and *Ulva*, with higher values in alkaline than in acidic waters. Values of δ^{13}C for specimens of the same genus collected in typical pH waters are mostly overlapped between alkaline and acidic seawaters. Non-significant differences in δ^{13}C values were observed for *Grateloupia, Hypnea*, and *Polysiphonia* concerning pH-type waters.

We analyzed the carbon uptake strategies on macroalgal assemblages as a function of environmental factors like temperature, pH, and salinity (Fig. 8). The temperature and salinity non-significantly explained the δ^{13}C macroalgal variability. A poor but significant correlation was observed be-

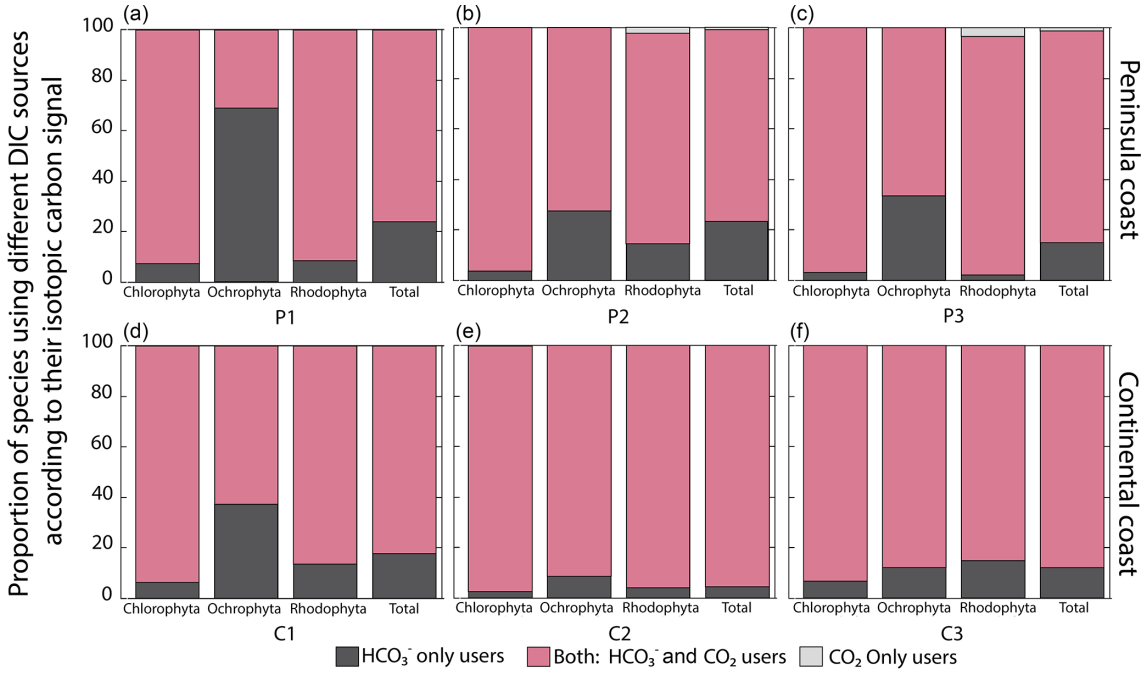

Figure 5. Proportion of species using different DIC sources according to their carbon uptake strategies: HCO_3^- only users (CO_2 concentrating mechanism active), users of both sources (HCO_3^- and CO_2), and CO_2 only users (non-CO_2 concentrating mechanism active) on the coast along the GC.

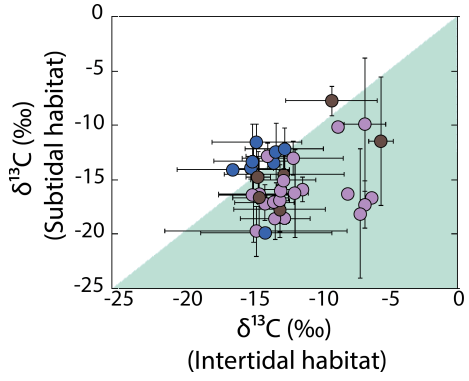

Figure 6. Variability in δ^{13}C values in macroalgae specimens for the most representative genera as a function of habitat features (emersion level). Blue circles represent the genus Chlorophyta, brown circles represent the genus Ochrophyta, and purple circles represent the genus Rhodophyta.

tween δ^{13}C and pH ($R^2 = 0.04$) (Table 4). The proportion of specimens with a strategy of only HCO_3^- use was different between environmental factors and taxa (previously described). For example, Ochrophyta showed the highest proportion (35 %) in colder temperatures, in pH alkaline (31 %), and in a typical salinity regimen (27 %). Chlorophyta was enhanced to 30 % in acid pH, and Rhodophyta recorded 21 % in normal seawater. The opposite strategy (only use of dissolved CO_2) was observed only in Rhodophyta. The highest percentage was observed in the estuarine salinity regimen (10 %).

3.5 Variation latitudinal of δ^{13}C macroalgae

The δ^{13}C macroalgal variation in the GC biogeography was evaluated by linear regression analysis between δ^{13}C values along the 9° latitude of both GC coastlines. A non-significant latitudinal trend was observed for datasets, but for the three phyla's most representative genera, δ^{13}C values correlated with latitude (Fig. 9). In Chlorophyta, with the higher genera number, δ^{13}C values increased with latitude, with low but significant correlation. Contrarily, in Ochrophyta and Rhodophyta specimens, the δ^{13}C values decreased non-significantly with latitude.

In the most representative morphofunctional groups, significant correlations ($p < 0.001$) were observed for δ^{13}C macroalgae versus latitude (Fig. 10). Representative morphofunctional groups of Chlorophyta (e.g., C-Tubular, C-Filamentous uniseriate) showed a positive correlation, while those belonging to Ochrophyta (e.g., O-Thick leathery) and Rhodophyta (e.g., R-Larger-sized corticated) showed a negative trend with latitude.

3.6 Analyses of δ^{13}C macroalgal variability

The δ^{13}C macroalgal variability was analyzed as a function of the life-form and environmental factors. Firstly, simple linear regression analyses were performed to evaluate the de-

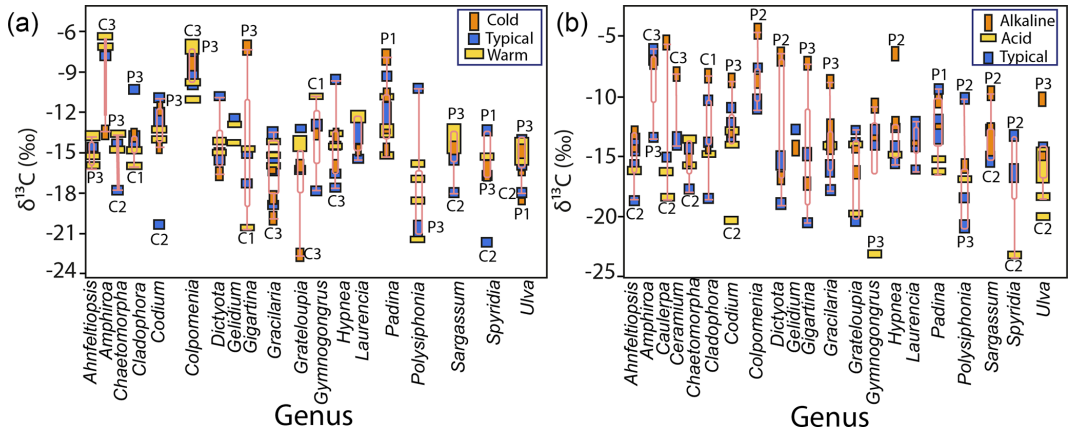

Figure 7. Variability in δ^{13}C values in macroalgae specimens for the most representative genera as a function of temperature **(a)** and pH **(b)** ranges in samples collected along the Gulf of California coastline.

Table 4. Summary of the estimated regression coefficients for each simple linear regression analysis and of the constant of fitted regression models. Estimated regression coefficients include degree of freedom for the error (DFE), root-mean-square error (RMSE), coefficient of determination (R^2) and the adjusted R^2 statistics, Mallow's Cp criterion (Cp), Akaike information criterion (AIC), Bayesian information criterion (BIC) minimum, F ratio test, and p value for the test (prob > F). Model information includes value of the constant a (δ^{13}C, ‰), standard error (SE), t ratio, and prob > $|t|$ (values * are significant).

	Estimated regression coefficients									Model constant (a)			
Independent variables	DFE	RMSE	R^2	Adjust R^2	Cp	AIC	BIC	F ratio	Prob > F	δ^{13}C (‰)	SE	t ratio	Prob > $\|t\|$
Inherent macroalgae properties													
Phyla	806	3.66	0.08	0.07	3	4401	4420	33.1	< 0.0001**	−13.98	0.13	−107.4	< 0.0001**
Morphofunctional	788	3.10	0.35	0.34	21	4149	4251	21.6	< 0.0001**	−14.21	0.35	−40.80	< 0.0001**
Genus	746	2.92	0.46	0.41	63	4104	4393	10.1	< 0.0001**	−14.71	0.23	−62.64	< 0.0001*
Species	641	2.79	0.57	0.46	168	4195	4898	5.2	< 0.0001**	−14.60	0.16	−93.22	< 0.0001**
Biogeographical collection zone													
GC coastline	807	3.79	0.01	0.01	2	4456	4470	7.4	0.0067*	−13.97	0.13	−104.5	< 0.0001**
Coastal sector	803	3.73	0.05	0.04	6	4433	4465	7.9	< 0.0001*	−14.12	0.16	−90.85	< 0.0001**
Latitude	807	3.80	0.00	0.00	2	4462	4476	1.5	0.23	−12.25	1.41	−8.71	< 0.0001**
Longitude	807	3.81	0.00	−0.00	2	4463	4477	0.1	0.80	−15.44	5.83	−2.65	0.0082*
Habitat features													
Substrate	807	3.80	0.00	0.00	2	4460	4474	3.2	0.08	−13.82	0.15	−92.06	< 0.0001*
Hydrodynamic	807	3.80	0.00	0.00	2	4462	4476	1.3	0.26	−13.88	0.15	−95.00	< 0.0001**
Emersion level	807	3.69	0.06	0.06	2	4412	4427	52.2	< 0.0001**	−14.05	0.13	−107.6	< 0.0001**
Environmental conditions													
Temperature	802	3.70	0.01	0.01	2	4390	4404	5.4	0.0207*	−16.11	0.96	−16.78	< 0.0001*
pH	807	3.73	0.04	0.04	2	4430	4444	33.4	< 0.0001**	−32.45	3.21	−10.13	< 0.0001**
Salinity	806	3.80	0.00	−0.00	2	4456	4470	0.9	0.34	−15.77	1.91	−8.27	< 0.0001**

* $p < 0.05$, ** $p < 0.0001$.

pendent variable's prediction power (δ^{13}C macroalgal variable) as a function of several independent variables controlling the main macroalgae photosynthesis drivers (light, DIC, and inorganic nutrients). Regression coefficients were estimated for each fitted regression model, which are used as indicators of the quality of the regression (Burnham and Anderson, 2002; Draper and Smith, 1998) as was described in Methods; however, the description of our results focused on the coefficients of determination (R^2 and adjusted R^2). The coefficient R^2 describes the relationship between the independent variables X_i with the dependent variable Y (δ^{13}C macroalgal values). R^2 is interpreted as the percent of contribution to the δ^{13}C variability. In comparison, the adjusted R^2 statistics compensate for possible confounding effects between variables.

Results of the analysis of the relationships between δ^{13}C with each independent variable are summarized in Table 4. Phyla explain only 8 % variability regarding the inher-

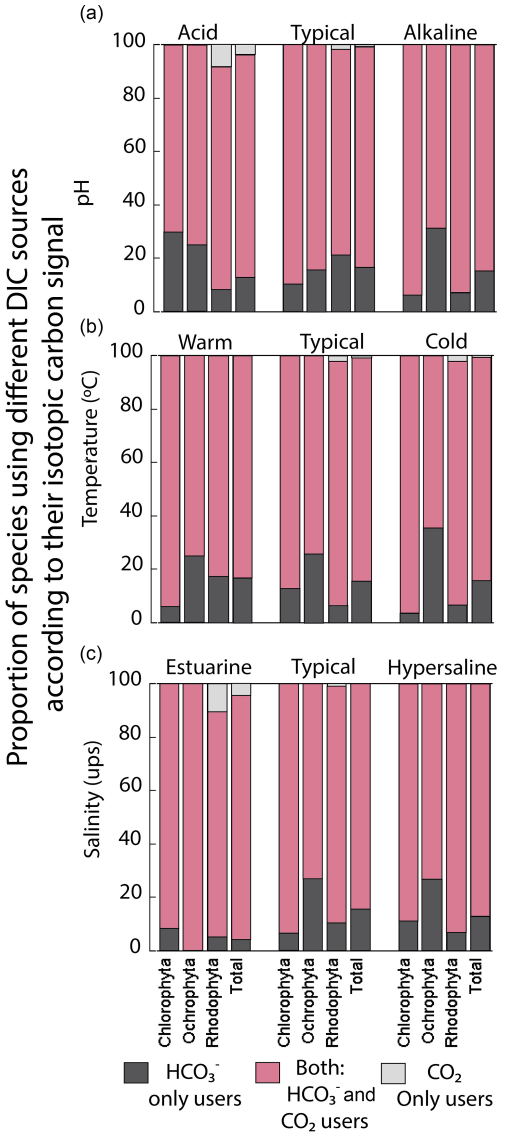

Figure 8. Proportion of species using different DIC sources according to their carbon assimilation strategies: HCO_3^- only users (CO_2 concentrating mechanism active), users of both sources (HCO_3^- and CO_2), and CO_2 only users (non-CO_2 concentrating mechanism active) as a function of **(a)** pH ranges, **(b)** temperature ranges, and **(c)** salinity ranges.

ent macroalgae properties, the morphofunctional properties 35 %, genera 46 %, and species 57 %.

The biogeographical collection zone, featured by coastline (continental versus peninsular) and coastal sectors (C1–C3 and P1–P3), explained a maximum of 5 % variability. Only the emersion level (6 %) contributed to the δ^{13}C variability related to the habitat features. The contribution of the seawater's environmental conditions was marginal for pH (4 %) and negligible for temperature and salinity. A marginal reduction in the percentage of contribution was observed for phyla (1 %) and morphofunctional properties (1 %), but it was significant for genera (5 %) and species (10 %).

Multiple regression analyses were also performed to interpret the complex relationships among δ^{13}C macroalgae, considering the life-forms (morphofunctional properties and taxa by genus) and their responses to environmental parameters. Results for the fitted regression models performed for morphofunctional groups (Table 5) and genera (Table 6) evidenced that the effect of the coastal sector and pH ranges on the δ^{13}C macroalgae increased the contribution by 9 %–10 % for each one. The emersion level increased by 5 %–6 %, the contribution with respect to the individual effect of morphofunctional group and genus, and the temperature and pH by 1 % and 3 %, respectively, while salinity decreased by 1 %–2 %. The combined effect of the biogeographical collection zone (e.g., coastline sector) and morphofunctional group (Table 5) and genus (Table 7) increased in 11 %–12 %.

Considering the combined effect of the coastline sector + habitat features for morphofunctional group or genus (Table 7), the full model showed R^2 values of 0.60 and 0.71. In contrast, coastline sector + environmental conditions + morphofunctional group or genus the R^2 increased to 0.62 and 0.72, respectively. The interactive explanations of environmental factors increased the explanation percentage of δ^{13}C variability; however, these contributions were significantly lower than those explained by life-forms, such as the morphofunctional properties and taxa by genus and species.

The combined effect of environmental conditions on the δ^{13}C variability was tested for the best-represented genera and morphological groups. Results evidenced that 9 of 21 morphological groups showed significant effects on the δ^{13}C variability (Table 8), five increasing and four decreasing the model constant of $\delta^{13}C = -14.2$ ‰. For example, for the O-Hollow with spherical or subspherical shape (+4.9 ‰) and R-Larger-sized articulated corallines (+6.3 ‰), the predicted values are -7.9 ± 0.8 ‰ and -9.2 ± 0.4 ‰. For R-Filamentous uniseriate and pluriseriate with erect thallus (−2.1 ‰) and C-Tubular (−1.6 ‰), the predicted values are -16.3 ± 0.5 ‰ and -15.8 ± 0.5 ‰, respectively. Regarding taxon, a significant effect was observed only in 13 genera, including *Colpomenia* (+5.4 ‰), *Amphiroa* (+6.8 ‰), and *Padina* (+2.2 ‰) increasing the signal and *Polysiphonia* (−3.7 ‰), *Gracilaria* (−0.9 ‰), and *Spyridia* (−1.4 ‰) decreasing the signal of the model constant (Table 9). In 33 species a significant effect on the δ^{13}C variability was observed, including *C. tuberculate* (+5.9 ‰), *C. sinuosa* (+4.4 ‰), *H. pannosa* (+4.4 ‰), *H. johnstonii* (+4.4 ‰), and *Amphiroa* spp. (+4.4 ‰ to 8.2 ‰) increasing the model constant $\delta^{13}C = -14.6$ ‰, and *Spyridia* sp. (−2.5 ‰), *G. filicina* (−2.3 ‰), *P. mollis* (−5.2 ‰), and *S. pacifica* (−19.2 ‰) decreasing the model constant (Table 10).

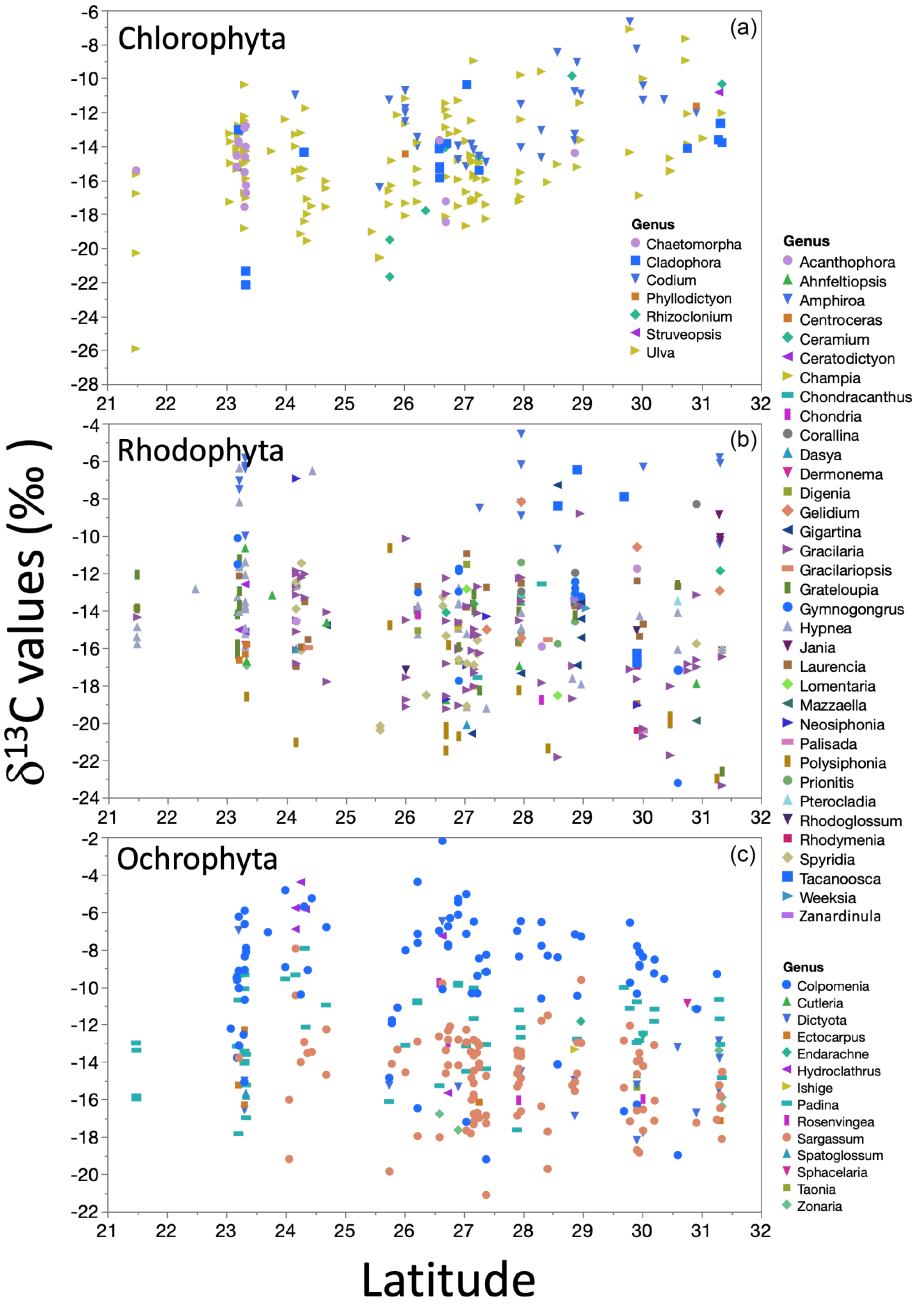

Figure 9. Trends in the δ^{13}C macroalgae in specimens for genera by taxa along the coastline of the Gulf of California as a function of latitudinal gradient.

3.7 Preliminary estimations of Δ^{13}C macroalgae

Concurrent analysis of surface seawater for alkalinity, proportions of the chemical species of DIC (CO_2, HCO_3^-, and CO_3^{2-}), and δ^{13}C DIC evidenced that δ^{13}C DIC in GC seawater averages 1.4 ± 0.4 ‰ (-1 ‰ to 4.9 ‰) (Fig. S1). In our preliminary data, the δ^{13}C-DIC seawater slightly (in 0.5 ‰) decreased during the rainy season in those zones influenced by river discharges along the continental coastline. Non-significant differences were observed among coastal sectors. The δ^{13}C-DIC values in GC seawater are comparable to the averages 1.4 ‰–1.6 ‰ reported for the surface seawaters in the eastern North Pacific in the 1970s–2000s (Hinger et al., 2010; Quay et al., 2003; Santos et al., 2011).

Based on the subtraction of δ^{13}C macroalgae to δ^{13}C-DIC seawater, the integrative discrimination factor against ^{13}C averaged 16.0 ± 3.1 ‰, 16.8 ± 4.3 ‰, and 14.0 ± 3.8 ‰ for phyla Chlorophyta, Rhodophyta, and Ochrophyta, re-

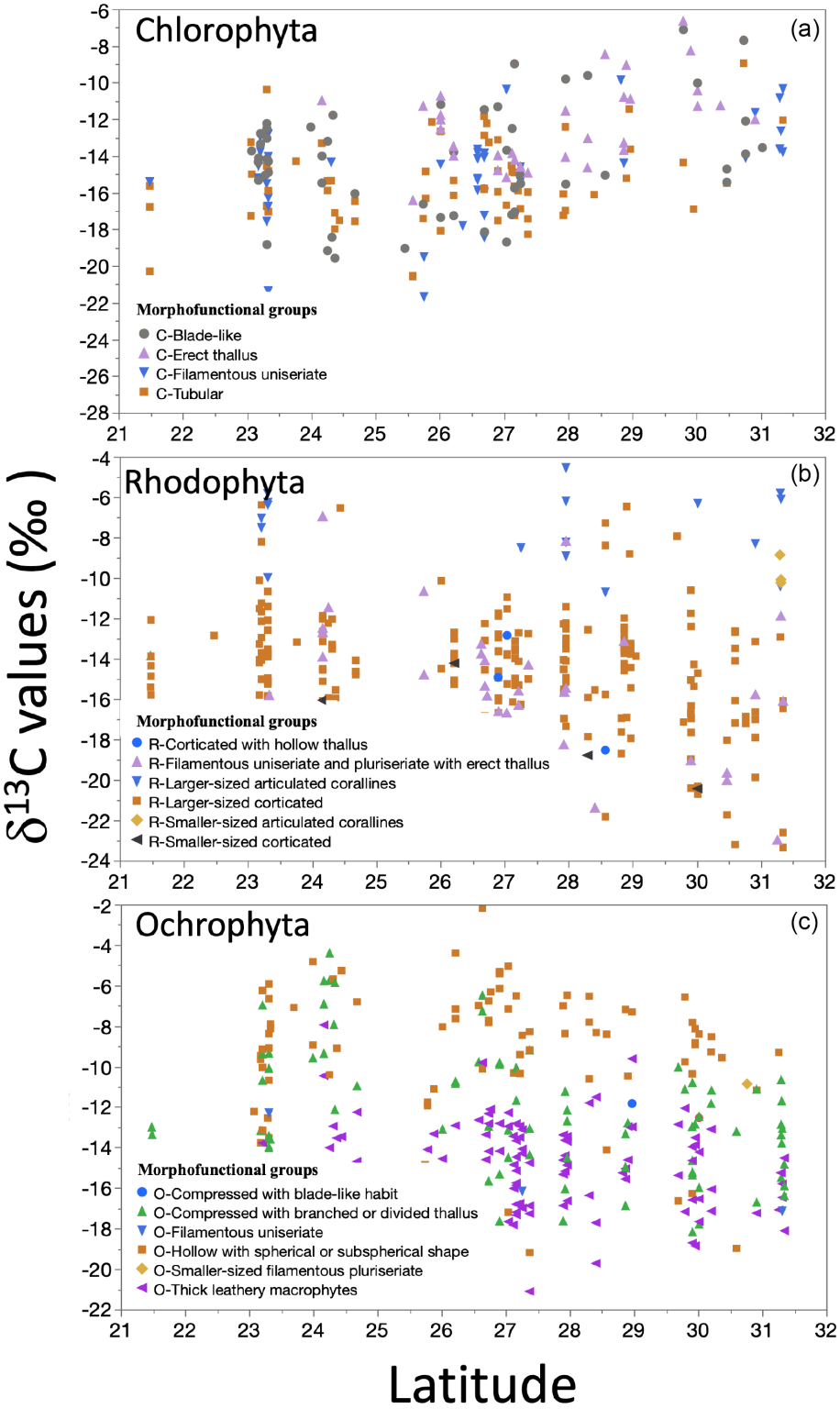

Figure 10. Trends in the δ^{13}C macroalgae in specimens for morphofunctional groups by taxa along the coastline of the Gulf of California as a function of latitudinal gradient.

Table 5. Summary of the estimated regression coefficients for each multivariate linear regression analysis and of their constant of fitted regression models performed in individuals binned by genus. Estimated regression coefficients include degree of freedom for the error (DFE), root-mean-square error (RMSE), coefficient of determination (R^2) and the adjusted R^2 statistics, Mallow's Cp criterion (Cp), Akaike information criterion (AIC), Bayesian information criterion (BIC) minimum, F ratio test, and p value for the test (prob > F). Model information includes value of the constant a (δ^{13}C, ‰), standard error (SE), t ratio, and prob > $|t|$ (values * are significant).

	Estimated regression coefficients									Model constant (a)			
Independent variables	DFE	RMSE	R^2	Adjust R^2	Cp	AIC	BIC	F ratio	Prob > F	δ^{13}C (‰)	SE	t ratio	Prob > $\|t\|$
Coastal sector	652	2.78	0.57	0.47	157	4169	4834	20.0	< 0.0001*	−17.52	0.64	−27.24	< 0.0001*
Substrate	711	2.90	0.49	0.42	98	4140	4577	0.4	0.52	−16.35	0.62	−26.20	< 0.0001*
Hydrodynamic	714	2.87	0.50	0.43	95	4120	4545	0.1	0.78	−16.53	0.64	−25.95	< 0.0001*
Emersion level	713	2.77	0.53	0.47	96	4060	4489	153.0	< 0.0001*	−16.65	0.60	−27.85	< 0.0001*
Temperature	695	2.81	0.50	0.43	109	4083	4564	98.4	< 0.0001*	−14.60	0.92	−15.91	< 0.0001*
Temperature ranges	686	2.87	0.49	0.40	118	4128	4645	97.7	< 0.0001*	−12.91	0.40	−31.97	< 0.0001*
pH	701	2.86	0.51	0.43	108	4134	4611	156.6	< 0.0001*	−28.57	2.69	−10.64	< 0.0001*
pH ranges	697	2.67	0.57	0.51	112	4028	4522	152.2	< 0.0001*	−16.39	0.58	−28.05	< 0.0001*
Salinity	697	2.89	0.50	0.42	111	4151	4640	162.2	< 0.0001*	−17.75	1.63	−10.88	< 0.0001*
Salinity ranges	721	2.91	0.47	0.41	86	4117	4504	167.8	< 0.0001*	−17.64	0.74	−23.68	< 0.0001*

Table 6. Summary of the estimated regression coefficients for each multivariate linear regression analysis and of their constant of fitted regression models performed in individuals binned by coastline sector and genus. Estimated regression coefficients include degree of freedom for the error (DFE), root-mean-square error (RMSE), coefficient of determination (R^2) and the adjusted R^2 statistics, Mallow's Cp criterion (Cp), Akaike information criterion (AIC), Bayesian information criterion (BIC) minimum, F ratio test, and p value for the test (prob > F). Model information includes value of the constant a (δ^{13}C, ‰), standard error (SE), t ratio, and prob > $|t|$ (values * are significant).

	Estimated regression coefficients									Model constant (a)			
Independent variables	DFE	RMSE	R^2	Adjust R^2	Cp	AIC	BIC	F ratio	Prob > F	δ^{13}C (‰)	SE	t ratio	Prob > $\|t\|$
Substrate	590	2.76	0.62	0.47	219	4287	5155	15.8	< 0.0001*	−17.08	0.66	−25.72	< 0.0001*
Hydrodynamic	592	2.73	0.62	0.49	217	4266	5128	18.6	< 0.0001*	−17.18	0.67	−25.70	< 0.0001*
Protection level	590	2.75	0.62	0.48	219	4285	5153	20.0	< 0.0001*	−17.51	0.64	−27.22	< 0.0001*
Emersion level	603	2.69	0.63	0.50	206	4217	5045	18.6	< 0.0001*	−17.47	0.64	−27.49	< 0.0001*
Temperature ranges	569	2.74	0.61	0.46	235	4293	5202	28.0	< 0.0001*	−13.73	0.45	−30.32	< 0.0001*
pH ranges	580	2.50	0.69	0.57	229	4155	5051	9.7	0.0019*	−16.88	0.62	−27.15	< 0.0001*
Salinity ranges	631	2.76	0.58	0.47	176	4183	4913	21.2	< 0.0001*	−18.30	0.79	−23.05	< 0.0001*

spectively. Five groups were identified as a function of the Δ^{13}C values: one for Chlorophyta ($\Delta^{13}C = 16.0 \pm 3.1$ ‰), two for Rhodophyta (16.6 ± 3.8 ‰ and 34.6 ± 1 ‰), and two for Ochrophyta (9.1 ± 1.7 ‰ and 15.7 ± 2.7 ‰) (Fig. S2). Values of Δ^{13}C were comparable to δ^{13}C of the thallus of macroalgae. Thus, δ^{13}C macroalgae reflect mainly the discrimination during carbon assimilation. Like δ^{13}C macroalgae, the Δ^{13}C values were subject to considerable variation.

4 Discussions

4.1 Explaining the δ^{13}C macroalgal variability

A high variability in the δ^{13}C values was revealed in the large inventory of macroalgae collected along the GC coastline. A linear regression analysis of the effects of life-forms revealed that the δ^{13}C variability in the macroalgal community is mainly explained by taxonomic (genus 46 %, species 57 %) and morphofunctional group (35 %). This result is consistent with the report of Lovelock et al. (2020), which found that 66 % of δ^{13}C variability was explained by taxonomy. Even so, the variability associated with each genus is not the same and can be classified in three groups: (1) high variability (e.g., *Schizymenia* = ±19.1 ‰), moderate variability (e.g., *Hydroclathrus* = ±7.3 ‰; *Amphiroa* = ±6.8 ‰), and low variability (e.g., *Gracilaria* = ±0.89; *Spyridia* = ±1.46 ‰). The observed δ^{13}C variability in this study is comparable with those reported in the literature, compiled in Table S4.

Most authors studying the isotopic composition of C in macroalgae have reported the high isotopic variability, which has been attributable to the taxon-specific photosynthetic DIC acquisition properties (Díaz-Pulido et al., 2016; Lovelock et al., 2020; Marconi et al., 2011; Mercado et al., 2009; Raven et al., 2002a; Stepien, 2015). Our study observed that the intrinsic characteristics of each morphofunctional group of macroalgae (e.g., thallus structure, growth form, branching pattern, and taxonomic affinities) also influence the δ^{13}C macroalgal signals. The thallus thickness influences the diffusion boundary layer on the surface of the macroalgae, where they carry out the absorption of essential ions and dissolved gases (Hurd, 2000; Sanford and Crawford, 2000). Thus, morphology can modulate the photosynthesis rates.

Table 7. Summary of the estimated regression coefficients for each multivariate linear regression analysis and of their constant of fitted regression models performed in individuals binned in coastline sector, habitat features, environmental conditions, and physiological state separately by morphofunctional group and genus. Estimated regression coefficients include degree of freedom for the error (DFE), root-mean-square error (RMSE), coefficient of determination (R^2) and the adjusted R^2 statistics, Mallow's Cp criterion (Cp), Akaike information criterion (AIC), Bayesian information criterion (BIC) minimum, F ratio test, and p value for the test (prob > F). Model information includes value of the constant a (δ^{13}C, ‰), standard error (SE), t ratio, and prob > $|t|$ (values * are significant).

	Estimated regression coefficients									Model constant (a)			
Full model	DFE	RMSE	R^2	Adjust R^2	Cp	AIC	BIC	F ratio	Prob > F	δ^{13}C (‰)	SE	t ratio	Prob > $\|t\|$
Coastline sector + habitat features + morphofunctional group													
I-Morphofunctional	593	2.79	0.60	0.46	216	4301	5160	20.8	< 0.0001*	−13.49	0.57	−23.52	< 0.0001*
Coastline sector + environmental conditions + morphofunctional group													
II-Morphofunctional	680	2.90	0.51	0.42	129	4189	4750	25.1	< 0.0001*	−13.42	0.54	−24.74	< 0.0001*
Coastline sector + habitat features + genus													
I-Genus	482	2.66	0.71	0.51	327	4565	5655	15.8	< 0.0001*	−16.93	0.73	−23.27	< 0.0001*
Coastline sector + environmental conditions + genus													
II-Genus	494	2.49	0.72	0.55	310	4374	5438	14.8	0.0001*	−13.55	0.64	−21.17	< 0.0001*

Table 8. Constant of fitted regression model explaining the δ^{13}C variability by morphofunctional groups. Model information includes value of the constant a (δ^{13}C, ‰), standard error (SE), t ratio, and prob > $|t|$. Only morphofunctional groups with significant effects are listed.

Term	Estimated	SE	Razón t	Prob > $\|t\|$
Model constant	−14.2	0.4	−40.80	< 0.0001**
R-Smaller-sized articulated corallines	4.5	1.7	2.58	0.0100*
O-Compressed with branched or divided thallus	1.2	0.5	2.66	0.0079*
C-Erect thallus	1.8	0.6	2.84	0.0046*
R-Larger-sized articulated corallines	6.3	0.8	7.95	< 0.0001*
O-Hollow with spherical or subspherical shape	5.0	0.5	10.51	< 0.0001*
R-Blade-like with one of the few layers of cells	−5.9	3.0	−1.98	0.0476*
C-Tubular	−1.6	0.5	−3.26	0.0012*∗
R-Filamentous uni-pluriseriate with erect thallus	−2.2	0.6	−3.92	< 0.0001*
R-Flattened macrophytes with cortication	−8.9	1.3	−7.10	< 0.0001*

* $p < 0.05$, ** $p < 0.0001$.

However, a non-biological or ecological explanation of the δ^{13}C variability, and therefore carbon use physiology, can be given in terms of morphology.

The δ^{13}C macroalgae depend on the carbon source (δ^{13}C DIC in seawater), the isotope discrimination during carbon assimilation in the photosynthesis ($\Delta^{13}C_p < 29$‰ in a variable degree), and the plant respiration ($\Delta^{13}C_r$ average ±2.3‰) (Carvalho et al., 2009a, b, 2010a; Carvalho and Eyre, 2011; Rautenberger et al., 2015). Comparatively, the $\Delta^{13}C_r$ value is relatively small regarding $\Delta^{13}C_p$. Thus, δ^{13}C macroalgal value is an integrative value of the isotope discrimination during DIC seawater assimilation ($\Delta^{13}C = (\delta^{13}$C-DIC seawater $- \delta^{13}$C macroalgae)) (Carvalho et al., 2009a). Based on the Δ^{13}C values, five groups were identified in our study: one for Chlorophyta ($\Delta^{13}C = 16.0 \pm 3.1$‰), two for Rhodophyta ($16.6 \pm 3.8$‰ and 34.6 ± 1‰), and two for Ochrophyta (9.1 ± 1.7‰ and 15.7 ± 2.7‰). Values of Δ^{13}C were comparable to δ^{13}C of the thallus of macroalgae. The δ^{13}C macroalgal values reflect the discrimination during carbon assimilation attributable to the taxon-specific photosynthetic DIC acquisition properties. Δ^{13}C macroalgal variability, captured in the δ^{13}C macroalgal signals, is related to the thickness of the boundary layer around the thallus (Raven et al., 1982), the leakage during carbon uptake (Maberly et al., 1992; Sharkey and Berry, 1985), photosynthetic intensity (Kübler and Raven, 1995, 1996; Wiencke and Fischer, 1990), and respiration rates (Carvalho et al., 2010a; Carvalho and Eyre, 2011; Rautenberger et al., 2015). All intrinsic properties are related to the life-form.

Many species that recorded high δ^{13}C values (and low Δ^{13}C values) were fleshy macroalgae that are characterized to be bloom-forming macroalgae belonging to genera *Ulva, Gracilaria, Cladophora, Spyridia*, and *Sargassum*

Table 9. Constant of fitted regression model explaining the δ^{13}C variability by genus. Model information includes value of the constant a (δ^{13}C, ‰), standard error (SE), t ratio and prob $> |t|$. Only genera with significant effects are enlisted.

Term	δ^{13}C, ‰ estimated	SE	t value	Prob $> \|t\|$
Model constant	−14.7	0.2	−62.64	< 0.0001**
Amphiroa	6.8	0.8	9.05	< 0.0001**
Codium	2.3	0.6	4.08	< 0.0001**
Colpomenia	5.4	0.4	14.02	< 0.0001*
Corallina	6.4	2.9	2.22	0.0269*
Gracilaria	−0.9	0.4	−2.18	0.0294*
Hydroclathrus	7.3	1.1	6.59	< 0.0001**
Jania	5	1.7	2.97	0.0031*
Padina	2.2	0.5	4.8	< 0.0001**
Polysiphonia	−3.7	0.8	−4.82	< 0.0001**
Schizymenia	−19.1	2.1	−9.33	< 0.0001**
Spyridia	−1.5	0.7	−2.10	0.0361*
Struveopsis	4.1	1.3	3.15	0.0017*
Tacanoosca	3.5	1.3	2.71	0.0070*

* $p < 0.05$, ** $p < 0.001$.

(Páez-Osuna et al., 2013; Valiela et al., 2018). It is not surprising that species with high photosynthetic activity and high relative growth rates (Hiraoka et al., 2020) have high carbon demand that results in lower isotopic discrimination against ^{13}C (Carvalho et al., 2010a, b; Cornelisen, et al., 2007; Kübler and Dungeon, 2015; Rautenberger et al., 2015). Bloom-forming macroalgae (e.g., *Ulva, Gracilaria, Sargassum*) have been remarked as facultative species capable of switching from C_3 to C_4 pathway (Valiela et al., 2018). C_4 pathway reduces photorespiration, the antagonist process of RuBisCo, enhancing the DIC assimilation in 25 %–40 % and increasing the δ^{13}C values (Bauwe et al., 2010; Ehleringer et al., 1991; Zabaleta et al., 2012). C4 pathway has more energy investment in CCMs than in RuBisCo protein content than C3 pathway (Young et al., 2016). Also, the reports of C4 or C4-like pathway features in algae have increased in the last years (Doubnerová and Ryšslavá, 2011; Roberts et al., 2007; Xu et al., 2012, 2013). For example, high activity of key enzymes of C4 metabolisms, such as pyruvate orthophosphate dikinase (PPDK), phosphoenolpyruvate carboxylase (PEPC), and phosphoenolpyruvate carboxykinase (PCK), has been described in many algae species. But the establishment of a true C4 pathway in marine algae is not clear since the massive changes in gene expression patterns seem to be incomplete, and it is suggested that many marine algae have high plasticity to use a combination of CCM to overcome DIC limitations (Doubnerová and Ryšlavá, 2011; Roberts et al., 2007; Xu et al., 2012, 2013). A stepwise model of the path from C3 to C4 photosynthesis is explained by Gowik and Westhoff (2011). More research is required on this topic considering the increasing frequency, intensity, and extension of bloom-forming macroalgae events worldwide (Teichberg et al., 2010; Valiela et al., 2018) and in México (Ochoa-Izaguirre et al., 2007; Ochoa-Izaguirre and Soto-Jiménez, 2015; Páez-Osuna et al., 2017).

Changes in the habitat features and environmental conditions, such as light intensity and DIC availability, influencing the growth rate and photosynthetic intensity, have a strong influence on δ^{13}C signal (Carvalho et al., 2007, 2009a; Carvalho and Eyre, 2011; Mackey et al., 2015; Rautenberger et al., 2015; Stepien, 2015). The light intensity is the external factor with more influence on the Δ^{13}C macroalgae due to the regulation of carbon assimilation intensity (Carvalho et al., 2009a, b; Cooper and DeNiro, 1989; Grice et al., 1996). Experimental studies found the light levels to be a critical factor affecting the δ^{13}C values. For example, under saturating light conditions, *Ulva* switched from a carbon uptake of HCO_3^- and CO_2 to increased HCO_3^- use (Rautenberger et al., 2015). Furthermore, field studies have shown that species growing in low-light habitats like deep subtidal zones tend to have more negative δ^{13}C values than those in higher-light environments (Cornwall et al., 2015; Díaz-Pulido et al., 2016; Hepburn et al., 2011; Marconi et al., 2011; Mercado et al., 2009; Stepien, 2015). In this study, intertidal specimens recorded less negative values than subtidal in most macroalgae genera. However, our study did not record the vertical effect in the δ^{13}C signal related to the light limitation because only shallow habitats (non-light limited) were studied.

The δ^{13}C-DIC seawater is reasonably uniform in surface seawater (−4.8 ‰ to 3.6 ‰, median 1.5 ‰), with δ^{13}C values for CO_2, HCO_3^-, and CO_3^{2-} nearly −10 ‰, −0.5 ‰, and 2 ‰, respectively (Kroopnick, 1985; Mook et al., 1974). Exceptions can be expected where variations in the salinity, alkalinity, and proportions of the chemical species of DIC (CO_2, HCO_3^-, or CO_3^{2-}) occur (e.g., in coastal environments influenced by river and groundwater discharges) (Carvalho et al., 2015; Chanton and Lewis, 1999; Hinger et al., 2010; Mook et al., 1974). Regarding DIC sources for macroalgae in the GC surface seawater, the availability, chemical proportions, and δ^{13}C DIC were also relatively constant and uniform. Thus, the influence of the δ^{13}C-DIC variations on the δ^{13}C macroalgal variability is negligible in the GC.

The effect of other environmental factors, such as salinity and pH, on δ^{13}C macroalgal signals was evaluated. Regarding salinity, the influence of freshwater discharge by rivers and groundwater decreases the δ^{13}C signal, which could be explained by the reduction in the salinity regimen that follows a decrease in δ^{13}C DIC in water (Hinger et al., 2010; Santos et al., 2011). In our study, a non-significant correlation between δ^{13}C macroalgae and salinity was observed.

Based on pH, differences in δ^{13}C were found only for a few genera (e.g., *Amphiroa, Colpomenia, Ulva, Spyridia*), with an increasing trend in the δ^{13}C values with pH increase, such as was reported by Maberly et al. (1992) and Raven et al. (2002b). Similar results were reported for Cornwall et al. (2017) in the field study, with the differential response of

Table 10. Constants of fitted regression model explaining the δ^{13}C variability by species. Model information includes value of the constant a (δ^{13}C, ‰), standard error (SE), t ratio, and prob > $|t|$. Only genera with significant effects are enlisted.

Term	δ^{13}C, ‰ estimated	SE	t value	Prob > $\|t\|$
Model constant	−14.6	0.2	−93.22	< 0.0001**
Amphiroa misakiensis	7.1	2.8	2.55	0.0110*
Amphiroa sp.	8.1	0.9	8.67	< 0.0001**
Amphiroa sp.2	6.6	1.6	4.1	< 0.0001**
Amphiroa sp. *3*	8.2	2.8	2.95	0.0033**
Caulerpa peltata	3.9	1.6	2.4	0.0165*
Cladophora microcladioides	−7.2	2	−3.64	0.0003**
Codium brandegeei	2.8	1.1	2.63	0.0088**
Codium simulans	3.2	0.9	3.41	0.0007**
Codium sp.	3	1.3	2.4	0.0167*
Colpomenia ramosa	3.2	1.4	2.27	0.0237*
Colpomenia sinuosa	4.4	1.1	4.17	< 0.0001**
Colpomenia sp.	3.6	0.9	4.27	< 0.0001**
Colpomenia tuberculata	5.9	0.4	15.45	< 0.0001**
Corallina vancouverensis	6.3	2.8	2.27	0.0238*
Grateloupia filicina	−2.4	1.1	−2.08	0.0382*
Halymenia actinophysa	−9.9	2.8	−3.57	0.0004**
Hydroclathrus clathratus	7.2	1.1	6.82	< 0.0001**
Hypnea johnstonii	3.4	1.3	2.74	0.0063**
Hypnea pannosa	2.8	1.3	2.24	0.0256*
Jania sp.	5	2	2.56	0.0106*
Padina durvillei	1.4	0.5	2.87	0.0043**
Padina sp.	3.5	0.7	4.77	< 0.0001**
Polysiphonia mollis	−5.2	1.1	−4.93	< 0.0001**
Polysiphonia sp.	−4.8	1.4	−3.44	0.0006**
Pyropia thuretii	−5.5	2.8	−1.98	0.0480*
Rhizoclonium riparium	−5.1	1.6	−3.15	0.0017**
Rhodymenia sp.	−4.1	2	−2.08	0.0380*
Schizymenia pacifica	−19.2	2	−9.76	< 0.0001**
Spyrida sp.	−2.5	1.3	−1.97	0.0496*
Struveopsis sp.	4	1.4	2.86	0.0044**
Tacanoosca uncinata	3.4	1.3	2.74	0.0062**
Ulva acanthophora	−1.2	0.6	−2.06	0.0399*
Ulva compressa	−3.2	1.4	−2.33	0.0203*

* $p < 0.05$, ** $p < 0.001$.

the δ^{13}C signals to pH among 19 species, in which only four species were sensitive to pH changes. A very weak but significant positive linear regression was observed between δ^{13}C and pH. Also, a decreasing trend in the δ^{13}C was recorded in the following order: alkaline > typical > acidic. According to Stepien (2015), the result of meta-analyses between pH drift experiments and δ^{13}C thresholds was positive only for Rhodophyta and Ochrophyta but not for Chlorophyta. About 86% of the Stepien metadata met the theoretical CCM assignation based on both parameters, with exceptions for species with $\delta^{13}C < -30$ ‰ that have been capable of raising pH to > 9. A strong association between pH compensation point and δ^{13}C was reported by Iñiguez et al. (2019) in three taxa of polar macroalgae. Environmental conditions may influence the δ^{13}C macroalgal values but not change the carbon use physiology in the macroalgae, which is most likely inherently species-specific.

4.2 Using δ^{13}C macroalgae to indicate the presence of an active CCM

In our study, the δ^{13}C macroalgal signals were used to evidence the presence of an active CCM. This tool was first used in macroalgal shallow communities of the GC. Most macroalgae species displayed δ^{13}C values that exhibit active CCMs. Then, macroalgae were classified into three strategies for DIC uptake, in agreement with the Maberly et al. (1992) and Raven et al. (2002a) thresholds: (1) CCM-only by active uptake HCO_3^- ($\delta^{13}C > -10$ ‰), (2) CCM active uptake HCO_3^- and diffusive uptake CO_2 ($\delta^{13}C < -11$ ‰ to -30 ‰), and (3) non-CCM CO_2 by diffusion only ($\delta^{13}C < -30$ ‰).

About 84 % of the analyzed specimens showed the facultative uptake of HCO_3^- and CO_2, the most common strategy identified in macroalgal shallow communities (Cornwall et al., 2015; Díaz-Pulido et al., 2016; Hepburn et al., 2011; Stepien, 2015). Based on the carbon uptake strategies, the most abundant macroalgae were those able to use both HCO_3^- and CO_2 using active uptake plus passive diffusion (strategy 2).

Macroalgae collected in GC also involved only HCO_3^- users (strategy 1) and those relying on diffusive CO_2 uptake (strategy 3). Photosynthesis that relies on CO_2 uptake (lack of CCM), the most primitive mechanism (Cerling et al., 1993), has fewer energy costs than HCO_3^- uptake, which requires complex machinery with a high operational cost (Giordano et al., 2005; Hopkinson et al., 2011, 2014; Raven and Beardall, 2016). The energy for macroalgae to uptake HCO_3^-, cross the plasma membrane, and convert to CO_2 for photosynthesis is obtained through irradiance (Cornelisen et al., 2007). Based on our sampling effort, focused on intertidal and shallow subtidal habitats featured by high light intensities, we expected high proportions of species with the carbon uptake strategy that use only HCO_3^-. Results evidenced that strategy 1 was recorded in specimens belonging to 58 species of 170 total species. The higher proportions of CCM species (HCO_3^- users) with high energetic requirements are explained by those elevated irradiances (Cornwall et al., 2015; Hepburn et al., 2011). Ochrophyta showed the highest proportion of species that depend only on HCO_3^- uptake on both coastlines in the southern region of GC (P1, C1). The low solubility of CO_2 is related to high temperatures in subtropical waters (Zeebe and Wolf-Gladrow, 2001) that impulse the development of CCM (Raven et al., 2002b) and by the high affinity to DIC by Ochrophyta, such as has been described before by Díaz-Pulido et al. (2016).

Only three non-calcifying species (*Schizymenia pacifica*, *Halymenia* sp., *Gigartina* sp.) belonging to Rhodophyta were CO_2-exclusive users ($\delta^{13}C = -33.2 \pm 1$ ‰). Based on measurements of pH drift, Murru and Sandgren (2004) reported *Schizymenia pacifica* and two species of *Halymenia* (e.g., *H. schizymenioides* and *H. gardner*) as restricted CO_2 users. Measurements of δ^{13}C in *Halymenia dilatata* confirmed the CO_2-restricted photosynthesis in specimens collected offshore in deep reefs of the Great Barrier Reef (Díaz-Pulido et al., 2016). Red macroalgae that lack CCM tend to inhabit low-light habitats like subtidal or low intertidal zones and are abundant in cold waters (Cornwall et al., 2015; Raven et al., 2002a). According to these authors, approximately 35 % of the total red algae tested globally are strictly CO_2 dependents. The percentage of macroalgae species representative of Arctic and Antarctic ecosystems that lack CCM is 42 %–60 % (Iñiguez et al., 2019; Raven et al., 2002b), 50 % for temperate waters of New Zealand (Hepburn et al., 2011), and up to 90 % found for a single site of Tasmania, Australia (Cornwall et al., 2015). Our study sampled 91 red macroalgae species (of 453 red macroalgae species reported in the GC; Pedroche and Sentíes, 2003), of which < 3 % were CO_2 dependents. This low percentage could be related to the fact that deep habitats (> 2 m depth low tide) were not explored in our surveys.

Few calcifying macroalgae species using HCO_3^- were also collected, including the genera *Amphiroa* (-7.8 ± 3.7 ‰) and *Jania* (-9.4 ± 0.7 ‰), both Rhodophyta with articulated form. *Padina*, a genus with less capacity to precipitate $CaCO_3$ (Iluz et al., 2017), displayed relatively high δ^{13}C values (-12.5 ± 2.4 ‰), suggesting the presence of CCM using HCO_3^-. Some species of *Padina* can use HCO_3^-, but their efficiency may differ from species to species (Enríquez and Rodríguez-Román, 2006; Raven et al., 2002a). Stepien (2015) reported a global mean of -14.8 ± 1.0 ‰ for calcifying species compared to -20.1 ± 0.3 ‰ for non-calcifying species. Calcifying macroalgae species showed a δ^{13}C signal indicative of HCO_3^- use, the same source described as the substrate for calcification (Digby, 1977; Roleda et al., 2012), and other sources like respiratory CO_2 for the calcifying process (Borowitzka and Larkum, 1976). Also, the boundary layers acidified by an excess of H^+ released as residual products of the calcification benefit the HCO_3^- uptake (Comeau et al., 2012; McConnaughey et al., 1997). Another possibility to explain high δ^{13}C values can also be related to the highly efficient light properties enhanced by the carbonate skeleton, resulting in an optimization of photosynthetic activity (Vásquez-Elizondo et al., 2017). Hofmann and Heesch (2018) reported high δ^{13}C values in eight rhodolith species (calcifying species) for the organic matter thallus and for thallus, including $CaCO_3$ structure collected in deep habitats (25–40 m) where light availability is limited. Because of the ocean acidification in progress, negative impacts are expected on calcifying organisms, and more attention as ecological sentinels is warranted in the GC.

Measurements of δ^{13}C signal are evidence of the presence or absence of CCMs in macroalgae and indicate carbon use physiology (Giordano et al., 2005). However, the isotopic signature may be inconclusive in determining the efficient use of one or more DIC species (CO_2 and HCO_3^-) (Roleda and Hurd, 2012). The preferential DIC uptake of macroalgae is assessed by pH drift experiments (Fernández et al., 2014, 2015; Hepburn et al., 2011; Narvarte et al., 2020; Roleda and Hurd, 2012). Also, it can be determined by simultaneously measuring the CO_2 uptake and O_2 production rates using membrane-inlet mass spectroscopy (MIMS) (Burlacot et al., 2020; Douchi et al., 2019). Macroalgae that are unable to raise the seawater pH to > 9.0 are primarily CO_2 users, while those that can raise the seawater pH > 9.0 (absence of CO_2) are HCO_3^- users (Roleda and Hurd, 2012). Those differences in the carbon uptake strategies can be easily deduced by pH drift experiments, which were not done in our study but are reported in the literature (Table S4). Also, the change in δ^{13}C signature within the range specific to a carbon use strategy (e.g., mixed HCO_3 and CO_2^- user) can be com-

plemented by simultaneous measurements of O_2 and CO_2 produced and consumed, respectively, using MIMS. For example, photosynthetic O_2 production in a certain macroalgal species with an active CCM preference (e.g., CO_2) is about 10 times higher than a non-active CCM (Burlacot et al., 2020).

Based on the δ^{13}C values, it is possible to assume that at least one basal CCM is active. However, it is not possible to discern what type of CCM is expressed in the organisms (e.g., direct HCO_3^- uptake by the anion-exchange protein – AE; Drechsler and Beer, 1991; Drechsler et al., 1993) or types of mitochondrial carbonic anhydrase (e.g., internal and external) that enhance the fixation of DIC by recycling mitochondrial CO_2 (Bowes, 1969; Sand-Jensen et al., 2020; Zabaleta et al., 2012). Also, the co-existence of different CCMs has been described for the same species (Axelsson et al., 1999; Xu et al., 2012), and it has even been described that different CCMs can operate simultaneously, generating different DIC contributions to RuBisCo internal pool (Rautenberger et al., 2015). The variety of CCMs and their combinations could contribute to the high δ^{13}C variability for the same species. In our field study, it is impossible to explain the variations in δ^{13}C or Δ^{13}C macroalgae relative to CCM or CA activity types. Controlled experiments, like those conducted by Carvalho and collaborators (e.g., Carvalho et al., 2009a, b, 2010a), are required to obtain this knowledge.

4.3 Variability in δ^{13}C macroalgae between the GC bioregions

Changes in the δ^{13}C signal with latitude, mainly related to the light and temperature, have been reported in the literature (Hofmann and Heesch, 2018; Lovelock et al., 2020; Marconi et al., 2011; Mercado et al., 2009; Stepien, 2015). For example, a negative correlation between latitude and δ^{13}C macroalgae was described by Stepien (2015). The authors concluded that the δ^{13}C signal increased by 0.09 ‰ for each latitude degree from the Equator. Hofmann and Heesch (2018) showed a robust decreasing latitudinal effect in δ^{13}C signals ($R^2 = 0.43 \delta^{13}C_{total}$ and 0.13, for $\delta^{13}C_{organic\text{-}tissue}$, $p = 0.001$) for rhodolite and macroalgae from coral reefs in Australia. In both cases, the latitude range is higher than what we tested (30 to 80° and from 10 to 45°, respectively). These differences on a large scale tend to be associated with a temperature effect (Stepien, 2015) and their effect on CO_2 solubility in seawater (Zeebe and Wolf-Gladrow, 2001). However, in our study, no geographical pattern in the δ^{13}C macroalgae was observed. Our linear regression analyses for latitudes showed a low but significant correlation for the dataset classified by morphofunctional group and genus – negative in the cases of Rhodophyta and Ochrophyta groups and positive for Chlorophyta.

Light is not limited along the GC latitudes. Most of the shallow habitats occupied by macroalgal communities in the GC were high-light environments. In agreement with the literature, the surface seawater temperature across the GC varies by only 1 °C annual mean (Escalante et al., 2013; Robles-Tamayo, 2018). However, larger temperature variations of 5–10 °C were recorded in the coastal waters across the GC bioregions in both climatic seasons. The combined effect of the coastline sector, habitat feature, and environmental condition for morphofunctional group or genus explained 60 %–62 % and 71 %–72 % of the δ^{13}C variability, respectively. Our analysis of variability for the best-represented morphological groups (e.g., R-Filamentous uniseriate and pluriseriate with erect thallus and C-Tubular) and genera (e.g., *Colpomenia*, *Padina*, *Polysiphonia*, and *Gracilaria*) revealed that certain life-forms are better monitors explaining the variability in δ^{13}C macroalgae (and Δ^{13}C values) than others. The δ^{13}C variability in morphological groups refers to change within a specific carbon use strategy but not change in the carbon use physiology that is inherently species-specific. The biological or ecological relevance of the δ^{13}C variability as a function of the morphology, in terms of the efficiency in the use of DIC and the isotope discrimination during carbon assimilation and respiration, must be investigated in species of the same genus but which are morphologically different or between the same morphological structures belonging to a different taxon.

The proportion of specimens with different carbon uptake strategies also showed regional variations. For example, the facultative uptake of HCO_3^- and CO_2 was dominant in the macroalgal shallow communities in the GC (60 % to 90 % of specimens). Exceptions were observed for Ochrophyta in the P1 (68 %) and C1 (37 %) regions, where the strategy using only HCO_3^- dominated, while the strategy based on the use of only CO_2 was observed in the peninsular coast in P2 and P3 for Rhodophyta with 2 %–3.3 %. Finally, the coastal sector C2 showed more negative δ^{13}C values in macroalgae specimens of the same genus compared to the peninsular coastline (P1–P3). Small but detectable changes were observed in the phylum distribution based on environmental conditions. For example, Ochrophyta showed the highest proportion (35 %) in colder temperature, in pH alkaline (31 %), and in typical salinity regimen (27 %), while Chlorophyta enhanced to 30 % in acid pH, and Rhodophyta recorded 21 % in normal seawater. The opposite strategy (only use of dissolved CO_2) was observed only in Rhodophyta. The highest percentage was observed in the estuarine salinity regimen (10 %). Again, more research is required to obtain valuable information on the physiological and environmental status of macroalgae.

5 Conclusions

In conclusion, we observed high δ^{13}C macroalgal variability in macroalgae communities in the Gulf of California, such

as reported in other worldwide marine ecosystems. The life-form is the principal cause of δ^{13}C macroalgal variability, which explains up to 57 %. Changes in habitat characteristics and environmental conditions also influence the δ^{13}C macroalgal variability within a specific carbon use strategy. Considering the combined effect of the life-form, coastline sector, and environmental conditions, the full model explains up to 72 % (genus) of the variability. The effects of the coastal sector, pH ranges, and emersion level were significant, while for salinity and temperature they were negligible.

Most macroalgae inhabiting in GC displayed the presence of CO_2 concentrating mechanisms to uptake HCO_3^- for photosynthesis, and 84 % of the total analyzed specimens were able to use both HCO_3^- and/or CO_2 employing active uptake plus passive diffusion (strategy 2: $-10 < \delta^{13}C > -30$ ‰). Specimens belonging to 58 species of 170 total species showed carbon uptake strategy 1 that uses only HCO_3^-. A higher proportion of CCM species (HCO_3^- users) was expected because we focused on intertidal and shallow subtidal habitats featured by high light intensities. Only three non-calcifying species (*Schizymenia pacifica*, *Halymenia* sp., *Gigartina* sp.) belonging to Rhodophyta (3 %) were CO_2-exclusive users (strategy 3: $\delta^{13}C < -30$ ‰). The low percentage of CO_2 dependents versus 40 %–90 % reported for temperate regions could be related to the shallow habitat sampled in our surveys (< 2 m depth low tide). The calcifying macroalgae genera *Amphiroa* and *Jania* using HCO_3^- (high δ^{13}C values) were present in the macroalgal communities in the GC. Because of the ongoing ocean acidification, these calcifying organisms constitute excellent ecological sentinels in the GC.

Finally, diverse authors have reported significant correlations between δ^{13}C signal and latitude, mainly related to the light and temperature. However, in our study's latitude range (21–31° N), the linear regression analyses showed a low correlation for the δ^{13}C macroalgal dataset classified by morphofunctional group and genus, which was negative for Rhodophyta and Ochrophyta and positive for Chlorophyta. Non-clear δ^{13}C macroalgal patterns occur along the GC latitudes. However, detectable changes were observed in the δ^{13}C macroalgae and the proportion of specimens with different carbon uptake strategies among coastal sectors. For example, the facultative uptake of HCO_3^- and CO_2 was dominant in the macroalgal shallow communities in the GC (60 % to 90 % of specimens), but in the P1 (68 %) and C1 (37 %) the use of only HCO_3^- was the dominant strategy.

Our research is the first approximation to understand the δ^{13}C macroalgal variability in one of the most diverse marine ecosystems in the world, the Gulf of California. We did not pretend to resolve the intricate processes controlling the variations in δ^{13}C or Δ^{13}C macroalgae during carbon assimilation and respiration and determine the isolated influence of each environmental factor. Despite the large dataset and corresponding statistical analyses, our study faces limitations due to research design and because no research on δ^{13}C macroalgal analysis was developed previously in the GC. The primary deficiency is the lack of pH drift experiments to discriminate δ^{13}C signal variations in the carbon uptake strategies to determine preferential DIC uptake of macroalgae (CO_2 or HCO_3^-). The second limitation concerns the lack of controlled experiments to discern what type of CCM is expressed in macroalgae (e.g., direct HCO_3^- uptake by the anion-exchange protein AE, types of mitochondrial AC, or the co-existence of different CCMs). Also, more research is required to assess the biological or ecological relevance of the δ^{13}C variability as a function of the morphology (e.g., DIC uptake efficiency and isotope discrimination during carbon assimilation and respiration). Future studies assessing the ability of macroalgae to use CO_2 and/or HCO_3^- can be assessed by pH drift experiments and MIMS in the cosmopolites' species and within genus with differences in the δ^{13}C values between species (e.g., *Ulva* and *Sargassum*). Finally, controlled experiments in laboratory and mesocosm type combined with field studies are required to elucidate what type of CCM is expressed in macroalgae. Even so, the δ^{13}C macroalgae were a good indicator to infer the presence or absence of CCMs, to identify the macroalgae lineages that could be in a competitive advantage based on their carbon uptake strategy, and to identify their geographical distribution along with GC. Under the current climate change conditions and their effects as ocean acidification progresses and the bloom-forming macroalgae events increase in Mexico and worldwide, the analysis of δ^{13}C macroalgae constitutes an excellent tool to help to predict the prevalence and shift of species in macroalgal communities which are focused on carbon metabolism. However, to obtain the maximum benefit from isotopic tools in the carbon-use strategy study, diverse and species-specific, it is necessary to use them in combination with other techniques referred to herein.

Data availability. Datasets are each permanently deposited. Further information can be found at https://www.proquest.com/openview/2060de58b217ca47495469b53ae2f347/1?pq-origsite=gscholar&cbl=4882998 (Soto-Jimenez et al., 2020).

Supplement. The supplement related to this article is available online at: https://doi.org/10.5194/bg-19-1-2022-supplement.

Author contributions. RVO participated in the collection, processing, and analysis of the samples as a part of his master's degree thesis. MJOI also participated in sample collections and identified macroalgae specimens. MFSJ coordinated the research, was the graduate thesis director, and prepared the manuscript with contributions from all co-authors.

Competing interests. The contact author has declared that neither they nor their co-authors have any competing interests.

Acknowledgements. The authors would like to thank Humberto Bojórquez-Leyva, Yovani Montaño-Ley, and Arcelia Cruz-López for their invaluable field and laboratory work assistance. Thanks to Sarahí Soto-Morales for the English revision. UNAM-PAPIIT IN206409 and IN208613 provided financial support, and UNAM-PASPA supported MF Soto-Jimenez for a sabbatical year. Thanks to CONACYT for a graduate fellowship to Roberto Velázquez-Ochoa.

Financial support. This research has been supported by the Dirección General de Asuntos del Personal Académico, Universidad Nacional Autónoma de México (grant nos. PAPIIT IN206409 and PAPIIT IN208613).

Review statement. This paper was edited by Aninda Mazumdar and reviewed by Matheus C. Carvalho, Michael Roleda, and one anonymous referee.

References

Abbot, I. A. and Hollenberg, G.: Marine algae of California, Standford University Press, California, 827 pp., 1976.

Aguilar-Rosas, L. E. and Aguilar-Rosas, R.: Ficogeografía de las algas pardas (Phaeophyta) de la península de Baja California, in: Biodiversidad Marina y Costera de México, Comisión Nacional Biodiversidad y Centro de Investigaciones de Quintana Roo, México, edited by: Salazar-Vallejo, S. I. and González, N. E., 197–206, 1993.

Aguilar-Rosas, L. E., Pedroche, F. F., and Zertuche-González, J. A.: Algas Marinas no nativas en la costa del Pacífico Mexicano. Especies acuáticas invasoras en México, Comisión Nacional para el Conocimiento y Uso de la Biodiversidad, México, 211–222, 2014.

Álvarez-Borrego, S.: Gulf of California, in: Ecosystems of the World, edited by: Ketchum, B. H., Estuaries and Enclosed Seas, Elsevier, Amsterdam, 427–449, 1983.

Anthony, K. R., Ridd, P. V., Orpin, A. R., Larcombe, P., and Lough, J.: Temporal variation of light availability in coastal benthic habitats: Effects of clouds, turbidity, and tides, Limnol. Oceanogr., 49, 2201–2211, https://doi.org/10.4319/lo.2004.49.6.2201, 2004.

Axelsson, L., Larsson, C., and Ryberg, H.: Affinity, capacity and oxygen sensitivity of two different mechanisms for bicarbonate utilization in *Ulva lactuca* L. (Chlorophyta), Plant Cell Environ., 22, 969–978, https://doi.org/10.1046/j.1365-3040.1999.00470.x, 1999.

Balata, D., Piazzi, L., and Rindi, F.: Testing a new classification of morphological functional groups of marine macroalgae for the detection of responses to stress, Mar. Biol., 158, 2459–2469, https://doi.org/10.1007/s00227-011-1747-y, 2011.

Bastidas-Salamanca, M., Gonzalez-Silvera, A., Millán-Núñez, R., Santamaria-del-Angel, E., and Frouin, R.: Bio-optical characteristics of the Northern Gulf of California during June 2008, Int. J. Oceanogr., 2014, 384618, https://doi.org/10.1155/2014/384618, 2014.

Bauwe, H., Hagemann, M., and Fernie, A. R.: Photorespiration: players, partners and origin, Trends Plant Sci., 15, 330–336, https://doi.org/10.1016/j.tplants.2010.03.006, 2010.

Beardall, J. and Giordano, M.: Ecological implications of microalgal and cyanobacterial CO_2 concentrating mechanisms, and their regulation, Funct. Plant Biol., 29, 335–347, https://doi.org/10.1071/PP01195, 2002.

Bold, C. H. and Wynne, J. M.: Introduction to the Algae: Structure and reproduction, Prentice-Hall, Incorporated, New Jersey, USA, 706 pp., 1978.

Borowitzka, M. A. and Larkum, A. W. D.: Calcification in green alga *Halimeda*. III. Sources of inorganic carbon for photosynthesis and calcification and a model of mechanism of calcification, J. Exp. Bot., 27, 879–893, 1976.

Bowes, G. W.: Carbonic anhydrase in marine algae, Plant Physiol., 44, 726–732, https://doi.org/10.1104/pp.44.5.726, 1969.

Bray, N. A.: Thermohaline circulation in the Gulf of California, J. Geophys. Res.-Oceans., 93, 4993–5020, https://doi.org/10.1029/JC093iC05p04993, 1988.

Brodeur, J. R., Chen, B., Su, J., Xu, Y. Y., Hussain, N., Scaboo, K. M., Zhang, Y., Testa, J. M., and Cai, W. J.: Chesapeake Bay inorganic carbon: Spatial distribution and seasonal variability, Front. Mar. Sci., 6, 1–17, https://doi.org/10.3389/fmars.2019.00099, 2019.

Brusca, R. C., Findley, L. T., Hastings, P. A., Hendrickx, M. E., Cosio, J. T., and van der Heiden, A. M.: Macrofaunal diversity in the Gulf of California, in: Biodiversity, ecosystems, and conservation in Northern Mexico, 2005.

Burlacot, A., Burlacot, F., Li-Beisson, Y., and Peltier, G.: Membrane inlet mass spectrometry: a powerful tool for algal research, Front. Plant Sci., 11, 1302, https://doi.org/10.3389/fmicb.2019.01356, 2020.

Burnham, K. P. and Anderson, D. R.: A practical information-theoretic approach, Model selection and multimodel inference, 2nd Edn., Springer, New York, 2002.

Carrillo, L. and Palacios-Hernández, E.: Seasonal evolution of the geostrophic circulation in the northern Gulf of California, Estuar. Coast. Shelf S., 54, 157–173, https://doi.org/10.1006/ecss.2001.0845, 2002.

Carvalho, M. C. and Eyre, B. D.: Carbon stable isotope discrimination during respiration in three seaweed species, Mar. Ecol.-Prog. Ser., 437, 41–49, https://doi.org/10.3354/meps09300, 2011.

Carvalho, M. C., Hayashizaki, K., Ogawa, H., and Kado, R.: Preliminary evidence of growth influence on carbon stable isotope composition of *Undaria pinnatifida*, Mar. Res. Indones., 32, 185–188, 2007.

Carvalho, M. C., Hayashizaki, K., and Ogawa, H.: Carbon stable isotope discrimination: a possible growth index for the kelp *Undaria pinnatifida*, Mar. Ecol.-Prog. Ser., 381, 71–82, https://doi.org/10.3354/meps07948, 2009a.

Carvalho, M. C., Hayashizaki, K. I., and Ogawa, H.: Short-term measurement of carbon stable isotope discrimination in photosynthesis and respiration by aquatic macrophytes, with marine macroalgal examples, J. Phycol., 45, 761–770, 2009b.

Carvalho, M. C., Hayashizaki, K., and Ogawa, H.: Effect of pH on the carbon stable isotope fractionation in photosynthesis by the kelp *Undaria pinnatifida*, Coast. Mar. Sci., 34, 135–139, 2010a.

Carvalho, M. C., Hayashizaki, K., and Ogawa, H.: Temperature effect on carbon isotopic discrimination by *Undaria pinnatifida* (Phaeophyta) in a closed experimental system, J. Phycol., 46, 1180–1186, https://doi.org/10.1111/j.1529-8817.2010.00895.x, 2010b.

Carvalho, M. C., Santos, I. R., Maher, D. T., Cyronak, T., McMahon, A., Schulz, K. G., and Eyre, B. D.: Drivers of carbon isotopic fractionation in a coral reef lagoon: Predominance of demand over supply, Geochim. Cosmochim. Ac., 153, 105–115, https://doi.org/10.1016/j.gca.2015.01.012, 2015.

Cerling, T. E., Wang, Y., and Quade, J.: Expansion of C_4 ecosystems as an indicator of global ecological change in the late Miocene, Nature, 361, 344–345, https://doi.org/10.1038/361344a0, 1993.

Chanton, J. P. and Lewis, F. G.: Plankton and dissolved inorganic carbon isotopic composition in a river-dominated estuary: Apalachicola Bay, Florida, Estuaries, 22, 575–583, https://doi.org/10.2307/1353045, 1999.

CNA (Comisión Nacional del Agua): Atlas del agua en México, available at: https://www.gob.mx/cms/uploads/attachment/file/259372/_2012_EAM2012.pdf, (last access: 5 November 2019) 2012.

Comeau, S., Carpenter, R. C., and Edmunds, P. J.: Coral reef calcifiers buffer their response to ocean acidification using both bicarbonate and carbonate, Proc. Bio. Sci., 280, 20122374, https://doi.org/10.1098/rspb.2012.2374, 2012.

Cooper, L. W. and DeNiro, M. J.: Stable carbon isotope variability in the seagrass *Posidonia oceanica*: Evidence for light intensity effects, Mar. Ecol.-Prog. Ser., 50, 225–229, 1989.

Cornelisen, C. D., Wing, S. R., Clark, K. L., Hamish Bowman, M., Frew, R. D., and Hurd, C. L.: Patterns in the $\delta^{13}C$ and $\delta^{15}N$ signature of *Ulva pertusa:* interaction between physical gradients and nutrient source pools, Limnol. Oceanogr., 52, 820–832, 2007.

Cornwall, C. E., Revill, A. T., and Hurd, C. L.: High prevalence of diffusive uptake of CO_2 by macroalgae in a temperate subtidal ecosystem, Photosynth. Res., 124, 181–190, https://doi.org/10.1007/s11120-015-0114-0, 2015.

Cornwall, C. E., Comeau, S., and McCulloch, M. T.: Coralline algae elevate pH at the site of calcification under ocean acidification, Glob. Change Biol., 23, 4245–4256, 2017.

Dawson, E. Y.: The marine algae of the Gulf of California, Allan Hancock Pac. Exped., 3, 189–453, 1944.

Dawson, E. Y.: Marine red algae of Pacific México. Part 2. *Cryptonemiales* (cont.), Allan Hancock Pac. Exped., 17, 241–397, 1954.

Dawson, E. Y.: How to know the seaweeds, W.M.C. Brown Co. Publishers, Dubuque, Iowa, USA, 197 pp., 1956.

Dawson, E. Y.: The marine red algae of Pacific Mexico, Part 4, Gigartinales, Allan Hancock Pac. Exped., 2, 191–343, 1961.

Dawson, E. Y.: Marine red algae of Pacific México. Part 7. *Ceramiales*: Ceramiaceae, Delesseriaceae, Allan Hancock Pac. Exped., 26, 1–207, 1962.

Dawson, E. Y.: Marine red algae of Pacific México. Part 8. *Ceramiales*: Dasyaceae, Rhodomelaceae, Nova Hedwigia, 6, 437–476, 1963.

Díaz-Pulido, G., Cornwall, C., Gartrell, P., Hurd, C., and Tran, D. V.: Strategies of dissolved inorganic carbon use in macroalgae across a gradient of terrestrial influence: implications for the Great Barrier Reef in the context of ocean acidification, Coral Reefs, 35, 1327–1341, https://doi.org/10.1007/s00338-016-1481-5, 2016.

Digby, P. S. B.: Growth and calcification in coralline algae, *Clathromorphum circumscriptum* and *Corallina officinalis*, and significance of pH in relation to precipitation, J. Mar. Biol. Assoc. UK, 57, 1095–109, https://doi.org/10.1017/S0025315400026151, 1977.

Doubnerová, V. and Ryšlavá, H.: What can enzymes of C_4 photosynthesis do for C_3 plants under stress?, Plant Sci., 180, 575–583, https://doi.org/10.1016/j.plantsci.2010.12.005, 2011.

Douchi, D., Liang, F., Cano, M., Xiong, W., Wang, B., Maness, P. C., Lindblad, P., and Yu, J.: Membrane-Inlet Mass Spectrometry enables a quantitative understanding of inorganic carbon uptake flux and carbon concentrating mechanisms in metabolically engineered cyanobacteria, Front. Microbiol., 10, 1356–1356, https://https://doi.org/10.3389/fmicb.2019.01356, 2019.

Draper, N. R. and Smith, H.: Applied regression analysis, Vol. 326, John Wiley and Sons, New Jersey, USA, 1–715, ISBN 0-471-17082-8, 1998.

Drechsler, Z. and Beer, S.: Utilization of inorganic carbon by *Ulva lactuca*, Plant Physiol., 97, 1439–1444, https://doi.org/10.1104/pp.97.4.1439, 1991.

Drechsler, Z., Sharkia, R., Cabantchik, Z. I., and Beer, S.: Bicarbonate uptake in the marine macroalga *Ulva* sp. is inhibited by classical probes of anion exchange by red blood cells, Planta, 191, 34–40, https://doi.org/10.1007/BF00240893, 1993.

Dreckmann, K. M.: El género *Gracilaria* (Gracilariaceae, Rhodophyta) en el Pacífico centro-sur mexicano, Monografías ficológicas, 1, 77–118, 2002.

Dudgeon, S. R., Davison, I. R., and Vadas, R. L.: Freezing tolerance in the intertidal red algae *Chondrus crispus* and *Mastocarpus stellatus:* Relative importance of acclimation and adaptation, Mar Biol., 106, 427–436, https://doi.org/10.1007/BF01344323, 1990.

Dudley, B. D., Barr, N. G., and Shima, J. S.: Influence of light intensity and nutrient source on $\delta^{13}C$ and $\delta^{15}N$ signatures in *Ulva pertusa*, Aquat. Biol., 9, 85–93, https://doi.org/10.3354/AB00241, 2010.

Ehleringer, J. R., Sage, R. F., Flanagan, L. B., and Pearcy, R. W.: Climate change and the evolution of C4 photosynthesis, Trends Ecol. Evol., 6, 95–99, https://doi.org/10.1073/pnas.1718988115, 1991.

Enríquez, S. and Rodríguez-Román, A.: Effect of water flow on the photosynthesis of three marine macrophytes from a fringing-reef lagoon, Mar. Ecol.-Prog. Ser., 323, 119–132, https://doi.org/10.3354/meps323119, 2006.

Escalante, F., Valdez-Holguín, J. E., Álvarez-Borrego, S., and Lara-Lara, J. R.: Temporal and spatial variation of sea surface temperature, chlorophyll a, and primary productivity in the Gulf of California, Cienc. Mar., 39, 203–215, 2013.

Espinoza-Avalos, J.: Macroalgas marinas del Golfo de California, Biodiversidad marina y costera de México, Comisión Nacional Biodiversidad, Centro de Investigaciones de Quintana Roo, México, edited by: Salazar-Vallejo, S. I. and González, N. E., 328–357, 1993.

Espinosa-Carreón, T. L. and Escobedo-Urías, D.: South region of the Gulf of California large marine ecosystem upwelling, fluxes of CO_2 and nutrients, Environ. Dev., 22, 42–51, https://doi.org/10.1016/j.envdev.2017.03.005, 2017.

Espinosa-Carreón, T. L. and Valdez-Holguín, E.: Variabilidad interanual de clorofila en el Golfo de California, Ecol. Appl., 6, 83–92, 2007.

Fernández, P. A., Hurd, C. L., and Roleda, M. Y.: Bicarbonate uptake via an anion exchange protein is the main mechanism of inorganic carbon acquisition by the giant kelp *Macrocystis pyrifera* (L aminariales, Phaeophyceae) under variable pH, J. Phycol., 50, 998–1008, https://https://doi.org/10.1111/jpy.12247, 2014.

Fernández, P. A., Roleda, M. Y., and Hurd, C. L.: Effects of ocean acidification on the photosynthetic performance, carbonic anhydrase activity and growth of the giant kelp *Macrocystis pyrifera*, Photosynth. Res., 124, 293–304, 2015.

Gateau, H., Solymosi, K., Marchand, J., and Schoefs, B.: Carotenoids of microalgae used in food industry and medicine, Mini-Rev. Med. Chem., 17, 1140–1172, https://doi.org/10.2174/1389557516666160808123841, 2017.

Gilbert, J. Y. and Allen, W. E.: The phytoplankton of the Gulf of California obtained by the "E.W. Scripps" in 1939 and 1940, J. Mar. Res., 5, 89–110, https://doi.org/10.1016/0022-0981(67)90008-1, 1943.

Giordano, M., Beardall, J., and Raven, J. A.: CO_2 concentrating mechanisms in algae: mechanisms, environmental modulation and evolution, Annu. Rev. Plant Biol., 66, 99–131, https://doi.org/10.1146/annurev.arplant.56.032604.144052, 2005.

Grice, A. M., Loneragan, N. R., and Dennison, W. C.: Light intensity and the interactions between physiology, morphology and stable isotope ratios in five species of seagrass, J. Exp. Mar. Biol. Ecol., 195, 91–110, https://doi.org/10.1016/0022-0981(95)00096-8, 1996.

Gowik, U. and Westhoff, P.: The path from C_3 to C_4 photosynthesis, Plant Physiol., 155, 56–63, https://doi.org/10.1104/pp.110.165308, 2011.

Harris, D., Horwáth, W. R., and Van Kessel, C.: Acid fumigation of soils to remove carbonates prior to total organic carbon or carbon-13 isotopic analysis, Soil Sci. Soc. Am. J., 65, 1853–1856, https://doi.org/10.2136/sssaj2001.1853, 2001.

Hepburn, C. D., Pritchard, D. W., Cornwall, C. E., McLeod, R. J., Beardall, J., Raven, J. A., and Hurd, C. L.: Diversity of carbon use strategies in a kelp forest community: implications for a high CO_2 ocean, Glob. Change Biol., 17, 2488–2497, https://doi.org/10.1111/j.1365-2486.2011.02411.x, 2011.

Hinger, E. N., Santos, G. M., Druffel, E. R. M., and Griffin, S.: Carbon isotope measurements of surface seawater from a time-series site off Southern California, Radiocarbon, 52, 69–89, 2010.

Hiraoka, M., Kinoshita, Y., Higa, M., Tsubaki, S., Monotilla, A. P., Onda, A., and Dan, A.: Fourfold daily growth rate in multicellular marine alga *Ulva meridionalis*, Sci. Rep.-UK, 10, 1–7, 2020.

Hofmann, L. C. and Heesch, S.: Latitudinal trends in stable isotope signatures and carbon-concentrating mechanisms of northeast Atlantic rhodoliths, Biogeosciences, 15, 6139–6149, https://doi.org/10.5194/bg-15-6139-2018, 2018.

Hopkinson, B. M., Dupont, C. L., Allen, A. E., and Morel, F. M. M.: Efficiency of the CO_2-concentrating mechanism of diatoms, P. Natl. Acad. Sci. USA, 108, 3830–3837, https://doi.org/10.1073/pnas.1018062108, 2011.

Hopkinson, B. M., Young, J. N., Tansik, A. L., and Binder, B. J.: The minimal CO_2 concentrating mechanism of *Prochlorococcus* MED4 is effective and efficient, Plant Physiol., 166, 2205–2217, https://doi.org/10.1104/pp.114.247049, 2014.

Hurd, C. L.: Water motion, marine macroalgal physiology and production, J. Phycol., 36, 453–472, https://doi.org/10.1046/j.1529-8817.2000.99139.x, 2000.

Iluz, D., Fermani, S., Ramot, M., Reggi, M., Caroselli, E., Prada, F., Dubinsky, Z., Goffredo, S., and Falin, G.: Calcifying response and recovery potential of the brown alga *Padina pavonica* under ocean acidification, ACS Earth Space Chem., 1, 316–323, https://doi.org/10.1021/acsearthspacechem.7b00051, 2017.

Iñiguez, C., Galmés, J., and Gordillo, F. J.: Rubisco carboxylation kinetics and inorganic carbon utilization in polar versus cold-temperate seaweeds, J. Exp. Bot., 70, 1283–1297, https://doi.org/10.1093/jxb/ery443, 2019.

Sand-Jensen, E. L., Maberly, S. C., and Gontero, B.: Insights on the functions and ecophysiological relevance of the diverse carbonic anhydrases in microalgae, Int. J. Mol. Sci., 21, 2922, https://doi.org/10.3390/ijms21082922, 2020.

Johansson, G. and Snoeijs, P.: Macroalgal photosynthetic responses to light in relation to thallus morphology and depth zonation, Mar. Ecol.-Prog. Ser., 244, 63–72, https://https://doi.org/10.3354/meps244063, 2002.

Kim, M. S., Lee, S. M., Kim, H. J., Lee, S. Y., Yoon, S. H., and Shin, K. H.: Carbon stable isotope ratios of new leaves of *Zostera marina* in the mid-latitude region: implications of seasonal variation in productivity, J. Exp. Mar. Biol. Ecol., 461, 286–296, https://doi.org/10.1016/j.jembe.2014.08.015, 2014.

Klenell, M., Snoeijs, P., and Pedersen, M.: Active carbon uptake in *Laminaria digitata* and *L. saccharina* (Phaeophyta) is driven by a proton pump in the plasma membrane, Hydrobiologia, 514, 41–53, https://doi.org/10.1023/B:hydr.0000018205.80186.3e, 2004.

Kroopnick, P. M.: The distribution of ^{13}C of ΣCO_2 in the world oceans, Deep-Sea Res. Pt. I, 32, 57–84, https://doi.org/10.1016/0198-0149(85)90017-2, 1985.

Kübler, J. E. and Davison, I. R.: High-temperature tolerance of photosynthesis in the red alga *Chondrus crispus*, Mar. Biol., 117, 327–335, https://doi.org/10.1007/BF00345678, 1993.

Kübler, J. E. and Dudgeon, S. R.: Predicting effects of ocean acidification and warming on algae lacking carbon concentrating mechanisms, PLoS One, 10, e0132806, https://doi.org/10.1371/journal.pone.0132806, 2015.

Kübler, J. E. and Raven, J. A.: The interaction between inorganic carbon acquisition and light supply in *Palmaria palmata* (Rhodophyta), J. Phycol., 31, 369–375, https://doi.org/10.1111/j.0022-3646.1995.00369.x, 1995.

Kübler, J. E. and Raven, J. A.: Inorganic carbon acquisition by red seaweeds grown under dynamic light regimes, Hydrobiologia, 326, 401–406, 1996.

Lapointe, B. E. and Duke, C. S.: Biochemical strategies for growth of *Gracilaria tikvahiae* (Rhodophyta) in relation to light intensity and nitrogen availability, J. Phycol., 20, 488–495, https://doi.org/10.1111/j.0022-3646.1984.00488.x, 1984.

Littler, M. M. and Arnold, K. E.: Primary productivity of marine macroalgal functional-form groups from

south-western North America, J. Phycol., 18, 307–311, https://doi.org/10.1111/j.1529-8817.1982.tb03188.x, 1982.

Littler, M. M. and Littler, D. S.: The evolution of thallus form and survival strategies in benthic marine macroalgae: field and laboratory tests of a functional form model, Am. Nat., 116, 25–44, 1980.

Lobban, C. S. and Harrison, P. J.: Seaweed ecology and physiology, Cambridge University Press, New York, USA, ISBN 9780511626210, 1–366, 1994.

Lovelock, C. E., Reef, R., Raven, J. A., and Pandolfi, J. M.: Regional variation in δ^{13}C of coral reef macroalgae, Limnol. Oceanogr., 65, 2291–2302, https://doi.org/10.1002/lno.11453, 2020.

Lluch-Cota, S. E., Aragón-Noriega, E. A., Arreguín-Sánchez, F., Aurioles-Gamboa, D., Bautista-Romero, J. J., Brusca, R. C., Cervantes-Duarte, R., Cortes-Altamirano, R., Del-MonteLuna, P., Esquivel-Herrera, A., Fernández, G., Hendrickx, M. E., Hernandez-Vazquez, S., Herrera-Cervantes, H., Kahru, M., Lavin, M., Lluch-Belda, D., Lluch-Cota, D. B., López-Martínez, J., Marinone, S. G., Nevarez-Martinez, M. O., Ortega-García, S., Palacios-Castro, E., Pares-Sierra, A., Ponce-Díaz, G., Ramirez-Rodríguez, M., Salinas-Zavala, C. A., Schwartzlose, R. A., and Sierra-Beltrán, A. P.: The Gulf of California: Review of ecosystem status and sustainability challenges, Prog. Oceanogr., 73, 1–26, https://doi.org/10.1016/j.pocean.2007.01.013, 2007.

Maberly, S. C., Raven, J. A., and Johnston, A. M.: Discrimination between ^{12}C and ^{13}C by marine plants, Oecologia, 91, 481–492, https://doi.org/10.1007/BF00650320, 1992.

Mackey, A. P., Hyndes, G. A., Carvalho, M. C., and Eyre, B. D.: Physical and biogeochemical correlates of spatio-temporal variation in the δ^{13}C of marine macroalgae, Estuar. Coast. Shelf S., 157, 7–18, https://doi.org/10.1016/j.ecss.2014.12.040, 2015.

Madsen, T. V. and Maberly, S. C.: High internal resistance to CO_2 uptake by submerged macrophytes that use HCO_3^-: measurements in air, nitrogen and helium, Photosynth. Res., 77, 183–190, https://doi.org/10.1023/A:1025813515956, 2003.

Marinone, S. G.: A note on "Why does the Ballenas Channel have the coldest SST in the Gulf of California?", Geophys. Res. Lett., 34, L02607, https://doi.org/10.1029/2006GL028589, 2007.

Marinone, S. G. and Lavín, M. F.: Residual flow and mixing in the large islands' region of the central Gulf of California: Nonlinear processes in geophysical fluid dynamics, Springer, Dordrecht, https://doi.org/10.1007/978-94-010-0074-1_13, 2003.

Marconi, M., Giordano, M., and Raven, J. A.: Impact of taxonomy, geography and depth on the δ^{13}C and δ^{15}N variation in a large collection of macroalgae, J. Phycol., 47, 1023–1035, https://doi.org/10.1111/j.1529-8817.2011.01045.x, 2011.

Martínez-Díaz-de-León, A.: Upper-ocean circulation patterns in the Northern Gulf of California, expressed in Ers-2 synthetic aperture radar imagery, Cienc. Mar., 27, 209–221, https://doi.org/10.7773/cm.v27i2.465, 2001.

Martínez-Díaz-de-León, A., Pacheco-Ruíz, I., Delgadillo-Hinojosa, F., Zertuche-González, J. A., Chee-Barragán, A., Blanco-Betancourt, R., Guzmán-Calderón, J. M., and Gálvez-Telles, A.: Spatial and temporal variability of the sea surface temperature in the Ballenas-Salsipuedes Channel (central Gulf of California), J. Geophys. Res.-Oceans, 111, C02008, https://doi.org/10.1029/2005JC002940, 2006.

Masojidek, J., Kopecká, J., Koblížek, M., and Torzillo, G.: The xanthophyll cycle in green algae (Chlorophyta): its role in the photosynthetic apparatus, Plant Biol., 6, 342–349, https://doi.org/10.1055/s-2004-820884, 2004.

McConnaughey, T. A., Burdett, J., Whelan, J. F., and Paull, C. K.: Carbon isotopes in biological carbonates: respiration and photosynthesis, Geochim. Cosmochim. Ac., 61, 611–622, https://doi.org/10.1016/S0016-7037(96)00361-4, 1997.

Mercado, J. M., De los Santos, C. B., Pérez-Lloréns, J. L., and Vergara, J. J.: Carbon isotopic fractionation in macroalgae from Cadiz Bay (Southern Spain): comparison with other bio-geographic regions, Estuar. Coast. Shelf S., 85, 449–458, https://doi.org/10.1016/j.ecss.2009.09.005, 2009.

Mook, W. G., Bommerson, J. C., and Staverman, W. H.: Carbon isotope fractionation between dissolved bicarbonate and gaseous carbon dioxide, Earth Planet. Sc. Lett., 22, 169–176, https://doi.org/10.1016/0012-821X(74)90078-8, 1974.

Murru, M. and Sandgren, C. D.: Habitat matters for inorganic carbon acquisition in 38 species of red macroalgae (Rhodophyta) from Puget Sound, Washington, USA, J. Phycol., 40, 837–845, https://doi.org/10.1111/j.1529-8817.2004.03182.x, 2004.

Narvarte, B. C. V., Nelson, W. A., and Roleda, M. Y.: Inorganic carbon utilization of tropical calcifying macroalgae and the impacts of intensive mariculture-derived coastal acidification on the physiological performance of the rhodolith *Sporolithon* sp., Environ. Pollut., 266, 115344, https://doi.org/10.1016/j.envpol.2020.115344 , 2020.

Nielsen, S. L. and Sand-Jensen, K.: Allometric settling of maximal photosynthetic growth rate to surface/volume ratio, Limnol. Oceanogr., 35, 177–180, https://doi.org/10.4319/lo.1990.35.1.0177, 1990.

Norris, J. N.: The marine algae of the northern Gulf of California, PhD dissertation, University of California, Santa Barbara, 575 pp., 1975.

Norris, J. N.: Studies on *Gracilaria* Grev.(Gracilariaceae, Rhodophyta) from the Gulf of California, Mexico, Taxonomy of Economic Seaweeds, California Sea Grant College Program, California, Vol. I, 123–135, 1985.

Norris, J. N.: Marine algae of the northern Gulf of California: Chlorophyta and Phaoephyceae, Smithsonian Institution Scholarly Press, Washington DC, USA, no. 94, https://doi.org/10.5479/si.19382812.96, 2010.

Ochoa-Izaguirre, M. J. and Soto-Jiménez, M. F.: Variability in nitrogen stable isotope ratios of macroalgae: consequences for the identification of nitrogen sources, J. Phycol., 51, 46–65, https://doi.org/10.1111/jpy.12250, 2015.

Ochoa-Izaguirre, M. J., Aguilar-Rosas, R., and Aguilar-Rosas, L. E.: Catálogo de Macroalgas de las lagunas costeras de Sinaloa, Serie Lagunas Costeras, edited by: Páez-Osuna, F., UNAM, ICMyL, México, 117 pp., 2007.

Páez-Osuna, F., Piñón-Gimate, A., Ochoa-Izaguirre, M. J., Ruiz-Fernández, A. C., Ramírez-Reséndiz, G., and Alonso-Rodríguez, R.: Dominance patterns in macroalgal and phytoplankton biomass under different nutrient loads in subtropical coastal lagoons of the SE Gulf of California, Mar. Pollut. Bull., 77, 274–281, https://doi.org/10.1016/j.marpolbul.2013.09.048, 2013.

Páez-Osuna, F., Álvarez-Borrego, S., Ruíz-Fernández, A. C., García-Hernández, J., Jara-Marini, E., Bergés-Tiznado, M. E., Piñón-Gimate, A., Alonso-Rodríguez, R., Soto-Jiménez,

M. F., Frías-Espericueta, M. G., Ruelas-Inzunza, J. R., Green-Ruíz, C. R., Osuna-Martínez, C. C., and Sánchez-Cabeza, J. A.: Environmental status of the Gulf of California: a pollution review, Earth-Sci. Rev., 166, 181–205, https://doi.org/10.1016/j.earscirev.2016.09.015, 2017.

Pedroche, F. F. and Sentíes, A.: Ficología marina mexicana: Diversidad y Problemática actual, Hidrobiológica, 13, 23–32, 2003.

Quay, P., Sonnerup, R., Westby, T., Stutsman, J., and McNichol, A.: Changes in the $^{13}C/^{12}C$ of dissolved inorganic carbon in the ocean as a tracer of anthropogenic CO_2 uptake, Global Biogeochem. Cy., 17, 1–20, https://doi.org/10.1029/2001GB001817, 2003.

Rautenberger, R., Fernández, P. A., Strittmatter, M., Heesch, S., Cornwall, C. E., Hurd, C. L., and Roleda, M. Y.: Saturating light and not increased carbon dioxide under ocean acidification drive photosynthesis and growth in *Ulva rigida* (Chlorophyta), Ecol. Evol., 5, 874–888, https://doi.org/10.1002/ece3.1382, 2015.

Raven, J., Beardall, J., and Griffiths, H.: Inorganic C-sources for *Lemanea*, *Cladophora*, and *Ranunculus* in a fast-flowing stream: measurements of gas exchange and of carbon isotope ratio and their ecological implications, Oecologia, 53, 68–78, https://https://doi.org/10.1007/BF00377138, 1982.

Raven, J. A. and Beardall, J.: The ins and outs of CO_2, J. Exp. Bot., 67, 1–13, https://doi.org/10.1093/jxb/erv451, 2016.

Raven, J. A., Johnston, A. M., Kübler, J. E., Korb, R. E., McInroy, S. G., Handley, L. L., Scrimgeour, C. M., Walker, D. I., Beardall, J., Clayton, M. N., Vanderklift, M., Fredriksen, S., and Dunton, K. H.: Seaweeds in cold seas: evolution and carbon acquisition, Ann. Bot., 90, 525–536, https://doi.org/10.1093/aob/mcf171, 2002a.

Raven, J. A., Johnshton, A. M., Kübler, J. E., Korb, R. E., Mclnroy, S. G., Handley, L. L., Scrimgeour, C. M., Walker, D. I., Beardall, J., Vanderklift, M., Fredriksen, S., and Dunton, K. H.: Mechanistic interpretation of carbon isotope discrimination by marine macroalgae and seagrasses, Funct. Plant Biol., 29, 355–378, https://doi.org/10.1071/PP01201, 2002b.

Raven, J. A., Ball, L. A., Beardall, J., Giordano, M., and Maberly, S. C.: Algae lacking carbon-concentrating mechanisms, Can. J. Bot., 83, 879–890, https://doi.org/10.1139/b05-074, 2005.

Roberts, K., Granum, E., Leegood, R. C., and Raven, J. A.: C_3 and C_4 pathways of photosynthetic carbon assimilation in marine diatoms are under genetic, not environmental control, Plant Physiol., 145, 230–235, https://doi.org/10.1104/pp.107.102616, 2007.

Robles-Tamayo, C. M., Valdez-Holguín, J. E., García-Morales, R., Figueroa-Preciado, G., Herrera-Cervantes, H., López-Martínez, J., and Enríquez-Ocaña, L. F.: Sea surface temperature (SST) variability of the eastern coastal zone of the gulf of California, Remote Sens., 10, 1434, https://doi.org/10.3390/rs10091434, 2018.

Roden, G. I.: Oceanographic and meteorological aspects of the Gulf of California, Pac. Sci., 12, 21–45, 1958.

Roden, G. I. and Emilsson, L.: Physical oceanography of the Gulf of California, Simposium Golfo de California, Universidad Nacional Autónoma de México, Mazatlán, Sinaloa, México, 1979.

Roden, G. I. and Groves, G. W.: Recent oceanographic investigations in the Gulf of California, J. Mar. Res., 18, 10–35, 1959.

Roleda, M. Y. and Hurd, C. L.: Seaweed responses to ocean acidification, in: Seaweed biology (Novel Insights into Ecophysiology, Ecology and Utilization), edited by: Caldwell, M. M., Heldmaier, G., Jackson, R. B., Lange, O. L., Mooney, H. A., Schulze, E.-D., and Sommer, U., Springer, Berlin, Heidelberg, 407–431, 2012.

Roleda, M. Y., Boyd, P. W., and Hurd, C. L.: Before ocean acidification: calcifier chemistry lessons, J. Phycol., 48, 840–843, 2012.

Rusnak, G. A., Fisher, R. L., and Shepard, F. P.: Bathymetry and faults of Gulf of California, in: Marine Geology of the Gulf of California: A symposium, edited by: van Andel, T. H. and Shor Jr., G. G., AAPG Memoir, Tulsa, OK, USA, 3, 59–75, https://doi.org/10.1306/M3359C3, 1964.

Sand-Jensen, K. and Gordon, D.: Differential ability of marine and freshwater macrophytes to utilize HCO_3^- and CO_2, Mar. Biol., 80, 247–253, https://doi.org/10.1111/j.1469-8137.1981.tb03198.x, 1984.

Sanford, L. P. and Crawford, S. M.: Mass transfer versus kinetic control of uptake across solid-water boundaries, Limnol. Oceanogr., 45, 1180–1186, https://doi.org/10.4319/lo.2000.45.5.1180, 2000.

Santamaría-del-Angel, E., Alvarez-Borrego, S., and Müller-Karger, F. E.: Gulf of California biogeographic regions based on coastal zone color scanner imagery, J. Geophys. Res., 99, 7411–7421, https://doi.org/10.1029/93JC02154, 1994.

Santos, G. M., Ferguson, J., Acaylar, K., Johnson, K. R., Griffin, S., and Druffel, E.: $\Delta^{14}C$ and $\delta^{13}C$ of seawater DIC as tracers of coastal upwelling: A 5-year time series from Southern California, Radiocarbon, 53, 669–677, https://doi.org/10.1017/S0033822200039126, 2011.

Setchell, W. and Gardner, N.: The marine algae of the Pacific Coast of North America. Part II Chlorophyceae, Univ. Calif. Publ. Bot., 8, 139–374, https://doi.org/10.5962/bhl.title.5719, 1920.

Setchell, W. and Gardner, N.: The marine algae: Expedition of the California Academy of Sciences to the Gulf of California in 1921, Proc. Calif. Acad. Sci., 4th series, California Academy of Sciences, San Francisco, CA, USA, 12, 695–949, 1924.

Sharkey, T. D. and Berry, J. A.: Carbon isotope fractionation of algae as influenced by an inducible CO_2 concentrating mechanism, Inorganic carbon uptake by aquatic photosynthetic organisms, American Society of Plant Physiologists, Rockville, MD, USA, 389–401, 1985.

Soto-Jimenez, M. F., Velázquez-Ochoa, R., and Ochoa Izaguirre, M. J.: Analysis of the variation of stable carbon isotopes in macroalgae communities from shallow marine habitats in the Gulf of California ecoregion, Earth and Space Science Open Archive ESSOAr, https://doi.org/10.1002/essoar.10504972.1, online first, 2020.

Stepien, C. C.: Impacts of geography, taxonomy and functional group on inorganic carbon use patterns in marine macrophytes, J. Ecol., 103, 1372–1383, https://doi.org/10.1111/1365-2745.12451, 2015.

Stroup, W. W., Milliken, G. A., Claassen, E. A., and Wolfinger, R. D.: SAS for mixed models: introduction and basic applications, SAS Institute, Cary, NC, USA, 1–48, 2018.

Teichberg, M., Fox, S. E., Olsen, Y. S., Valiela, I., Martinetto, P., Iribarne, O., Muto, E. Y., Petti, M. A., Cobrisier, T. N., Soto-Jiménez, M., Páez-Osuna, F., Castro, P., Freitas, H., Zitelli, A., Cardinaletti, M., and Tagliapietra, D.: Eutrophication and macroalgal blooms in temperate and tropical coastal waters: nutrient enrichment experiments with *Ulva* spp., Glob. Change Biol., 16, 2624–2637, https://doi.org/10.1111/j.1365-2486.2009.02108.x, 2010.

Valiela, I., Liu, D., Lloret, J., Chenoweth, K., and Hanacek, D.: Stable isotopic evidence of nitrogen sources and C_4 metabolism driving the world's largest macroalgal green tides in the Yellow Sea, Sci. Rep., 8, 1–12, https://doi.org/10.1038/s41598-018-35309-3, 2018.

Vásquez-Elizondo, R. M. and Enríquez, S.: Light absorption in coralline algae (Rhodophyta): a morphological and functional approach to understanding species distribution in a coral reef lagoon, Front. Mar. Sci., 4, 297, https://doi.org/10.3389/fmars.2017.00297, 2017.

Vásquez-Elizondo, R. M., Legaria-Moreno, Pérez-Castro, M. A., Krämer, W. E., Scheufen, T., Iglesias-Prieto, R., and Enríquez, S.: Absorptance determinations on multicellular tissues, Photosynth. Res., 132, 311–324, https://doi.org/10.1007/s11120-017-0395-6, 2017.

Velasco-Fuentes, O. V. and Marinone, S. G.: A numerical study of the Lagrangian circulation in the Gulf of California, J. Marine Syst., 22, 1–12, https://doi.org/10.1016/S0924-7963(98)00097-9, 1999.

Young, E. B. and Beardall, J.: Modulation of photosynthesis and inorganic carbon acquisition in a marine microalga by nitrogen, iron, and light availability, Can. J. Bot., 83, 917–928, https://doi.org/10.1139/b05-081, 2005.

Young, J. N., Heureux, A. M., Sharwood, R. E., Rickaby, R. E., Morel, F. M., and Whitney, S. M.: Large variation in the Rubisco kinetics of diatoms reveals diversity among their carbon-concentrating mechanisms, J. Exp. Bot., 67, 3445–3456, https://doi.org/10.1093/jxb/erw163, 2016.

Xu, J., Fan, X., Zhang, X., Xu, D., Mou, S., Cao, S., Zheng, Z., Miao, J., and Ye, N.: Evidence of coexistence of C_3 and C_4 photosynthetic pathways in a green-tide-forming alga, *Ulva prolifera*, PloS one, 7, e37438, https://doi.org/10.1371/journal.pone.0037438, 2012.

Xu, J., Zhang, X., Ye, N., Zheng, Z., Mou, S., Dong, M., Xu, D., and Miao, J.: Activities of principal photosynthetic enzymes in green macroalga *Ulva linza*: functional implication of C_4 pathway in CO_2 assimilation, Sci. China Life Sci., 56, 571–580, https://doi.org/10.1007/s11427-013-4489-x, 2013.

Wiencke, C. and Fischer, G.: Growth and stable carbon isotope composition of cold-water macroalgae in relation to light and temperature, Mar. Ecol.-Prog. Ser., 65, 283–292, 1990.

Wilkinson, T. E., Wiken, E., Creel, J. B., Hourigan, T. F., and Agardy, T.: Marine Ecoregions of North America, Commission of Environmental Cooperation, Montreal, Canada, Montreal, Canada, 1–177, 2009.

Zabaleta, E., Martin, M. V., and Braun, H. P.: A basal carbon concentrating mechanism in plants?, Plant Sci., 187, 97–104, https://doi.org/10.1016/j.plantsci.2012.02.001, 2012.

Zeebe, R. E. and Wolf-Gladrow, D.: CO_2 in seawater: equilibrium, kinetics, isotopes, No. 65, Gulf Professional Publishing, Elsevier Oceanography Series, Oxford, United Kingdom, 1–341, 2001.

Zeitzschel, B.: Primary productivity in the Gulf of California, Mar. Biol., 3, 201–207, https://doi.org/10.1007/BF00360952, 1969.

Zou, D., Xia, J., and Yang, Y.: Photosynthetic use of exogenous inorganic carbon in the agarophyte *Gracilaria lemaneiformis* (Rhodophyta), Aquaculture, 237, 421–431, https://doi.org/10.1016/j.aquaculture.2004.04.020, 2004.